

Quaternary International

Holocene palaeoenvironmental evolution of the southern margin of the Salpi lagoon (Apulia, Southern Italy)

--Manuscript Draft--

Manuscript Number:	QUATINT-D-22-00245
Article Type:	Regular Article
Keywords:	Holocene; Tavoliere coastal plain; Palaeoenvironmental reconstruction; Pollen; Ostracoda; Human impact
Abstract:	<p>A total of ten cores were drilled to understand the relationship between the palaeoenvironmental evolution of the southern margin of the Salpi lagoon (Tavoliere coastal plain, Apulia, Italy) and the development of settlements on its shores during the last part of the Holocene (Late Northgrippian to Late Meghalayan).</p> <p>Micropalaeontological, palynological, and sedimentological analyses revealed local and regional events, some of which have already been recognised in the northern part of the coastal plain, close to the archaeological site of Coppa Nevigata. Facies and micropalaeontological analyses show that the lagoon was partially connected to the sea between 6.2 ka BP and 4.2 ka BP. Between 4.2 ka BP and 2.4 ka BP, the area was characterised by marshes and swamps with restricted brackish lagoon conditions and permanent freshwater input. After 2.4 ka BP, the continuous freshwater influx from the Carapelle River determined the progradation of the floodplain and the closure of the lagoon, with the formation of the two coastal lakes of Lago Salso (north) and Lago Salpi (south). Pollen data show the expansion of halophytic herbs under local brackish conditions during the Early Meghalayan and the exponential spread of dryland herbs consistent with the closure of the basin. The emersion of the land during the Late Meghalayan allowed the intensive exploitation of the area and the development of a highly anthropogenic landscape. The development of the settlements of pre-Roman Salpia Vetus, Roman Salapia, and Medieval Salpi was mainly determined by the insalubrious condition of the surrounding marshes, due to the reduction in water depth and oscillations in salinity.</p>

1 **Holocene palaeoenvironmental evolution of the southern margin of the Salpi lagoon**
2 **(Apulia, Southern Italy)**

3 Davide Susini^{a,*}, Cristiano Vignola^{b,c}, Roberto Goffredo^d, Darian Marie Tottene^e, Alessia
4 Masi^{b,c}, Alessandra Smedile^f, Paolo Marco De Martini^f, Francesca Romana Cintif^f, Laura
5 Sadori^b, Luca Fortig^g, Girolamo Fiorentino^h, Andrea Sposato^a, Ilaria Mazzini^a

6 ^a Institute of Environmental Geology and Geoengineering, IGAG-CNR, Area della Ricerca di Roma 1,
7 Strada Provinciale 35d, 9 - 00100, Montelibretti, Rome, Italy

8 ^b Department of Environmental Biology, Sapienza University of Rome, Piazzale A. Moro 5, 00185, Rome,
9 Italy

10 ^c Palaeo-Science and History (PS&H) Independent Research Group, Max Planck Institute for the Science of
11 Human History, Kahlaische Strasse 10, 07745, Jena, Germany

12 ^d Dipartimento di Studi Umanistici, Lettere, Beni Culturali, Scienze della Formazione, Università di Foggia,
13 Via Arpi 176, 71121, Foggia, Italy

14 ^e Department of History and Classical Studies, McGill University, 855 Sherbrooke Street West, H3A 2T7,
15 Montreal, Quebec, Canada

16 ^f Istituto Nazionale di Geofisica e Vulcanologia, Via di Vigna Murata 605, 00143, Rome, Italy


17 ^g Department of Earth Sciences 'Ardito Desio', University of Milano, via Mangiagalli 34, 20133, Milan, Italy

18 ^h Dipartimento di Beni Culturali, Università del Salento, Via Dalmazio Birago 64, Lecce, Italy

19 * Corresponding author.

20 E-mail address: davide.susini@igag.cnr.it (D. Susini).

21 **Abstract**

22  total of ten cores were drilled to understand the relationship between the
23 palaeoenvironmental evolution of the southern margin of the Salpi lagoon (Tavoliere coastal
24 plain, Apulia, Italy) and the development of settlements on its shores during the last part of
25 the Holocene (Late Northgrippian to Late Meghalayan). Micropalaeontological,
26 palynological, and sedimentological analyses revealed local and regional events, some of
27 which have already been recognised in the northern part of the coastal plain, close to the
28 archaeological site of **Coppa Navigata**. Facies and micropalaeontological analyses show that
29 the lagoon was partially connected to the sea between 6.2 ka BP and 4.2 ka BP. Between 4.2
30 ka BP and 2.4 ka BP, the area was characterised by marshes and swamps with restricted
31 brackish lagoon conditions and permanent freshwater input. After 2.4 ka BP, the continuous

32 freshwater influx from the Carapelle River determined the progradation of the floodplain
33 and the closure of the lagoon, with the formation of the two coastal lakes of Lago Salso
34 (north) and Lago Salpi (south). Pollen data show the expansion of halophytic herbs under
35 local brackish conditions during the Early Meghalayan and the exponential spread of
36 dryland herbs consistent with the closure of the basin. The emersion of the land during the
37 Late Meghalayan allowed the intensive exploitation of the area and the development of a
38 highly anthropogenic landscape. The development of the settlements of pre-Roman *Salpia*
39 *Vetus*, Roman *Salapia*, and Medieval *Salpi* was mainly determined by the insalubrious
40 condition of the surrounding marshes, due to the reduction in water depth and oscillations
41 in salinity.

42 **Keywords**

43 Holocene; Tavoliere coastal plain; Palaeoenvironmental reconstruction; Pollen; Ostracoda;
44 Human impact

45 **1. Introduction**

46 Coastal areas are well-studied, unique, and dynamic systems located between marine and
47 continental environments, and highly dependent on sedimentary and erosive processes,
48 glacio-eustatic oscillations, and tectonic regimes (Lambeck et al., 2011; Ruello et al., 2017;
49 Corrado et al., 2020; Buffardi et al., 2021). The sedimentary sequences preserved ~~within~~ these
50 environments represent high-resolution physical archives and are ~~considered contexts~~ of
51 primary interest in the Mediterranean region for the palaeoecological evolution of the Late
52 Quaternary ~~and the~~ complex interaction between anthropic and natural forcing mechanisms
53 (Sabatier et al., 2010; Ghilardi et al., 2013; Carmona et al., 2016; Cosentino et al., 2017; Natali
54 and Bianchini, 2018; Emmanouilidis et al., 2020; López-Belzunce et al., 2020; Di Lorenzo et
55 al., 2021). With so many examples ~~of natural contexts~~, as well as human strategies and
56 motives for inhabiting these coastal zones, their long-term evolution is neither obvious nor
57 assured. Therefore, reconstructing the palaeoenvironmental picture is crucial for ~~writing~~ the
58 history of these areas from prehistoric times to the present-day.

59 Indeed, the coastal wetlands of the Italian peninsula have been thoroughly studied through
60 multiproxy analyses (Mazzini et al., 1999; Amorosi et al., 2013; Sacchi et al., 2014; D'Orefice
61 et al., 2020; Pieruccini and Susini, 2020). In the Apulian region (Southern Italy), the most

62 important is the wetland of the Tavoliere Plain, also known as the Salpi lagoon, an area
63 densely settled and exploited since the Early Neolithic (Whitehouse, 2014, and references
64 therein). Earlier studies by Delano Smith and Morrison (1974) and Delano Smith (1976) at
65 Palude Frattarolo and Lago Salso (Fig. 1), on the north-eastern edge of the coastal plain,
66 revealed the presence of wetlands during the 1st cent. CE, south of the ~~ancient~~ port of
67 *Sipontum* and separated from the open sea by a sandy barrier. Investigations continued
68 mainly in the northern part of the coastal plain, focusing on the area surrounding the
69 archaeological site of Coppa Nevigata, a settlement inhabited from the Early Neolithic to
70 the Iron Age (Caldara et al., 2003; 2004). Here, palaeoenvironmental analyses showed that
71 the wetlands at the periphery of the settlement underwent several rapid changes during the
72 Bronze and Iron Ages due to anthropogenic activities (Caldara and Simone, 2005; 2012). ~~In~~
73 ~~contrast,~~ analyses within the lagoon basin showed a natural regressive trend of the wet
74 environment, gradually becoming dryland (Caldara and Simone, 2005; Di Rita et al., 2011).

75 ~~However,~~ there is little data available from the southern part of the coastal plain (Battista et
76 al., 1994; Caldara et al., 2002). ~~Archaeological fieldwork has been focused on the remains of~~
77 ~~the superimposed Roman town of Salapia and the Medieval city of Salpi~~ (Marin, 1973; De
78 Venuto et al., 2022). According to historical records, this sector of the coastal plain has been
79 inextricably linked to the Salpi lagoon. For instance, the historian Vitruvius writes about the
80 foundation of the Roman town of *Salapia* that the lagoon was transformed into a natural
81 harbour (*de Arch.* I.4.12). From its inception, this body of water was considered crucial for
82 the economic development, connections, and coastal character. Later historical sources, such
83 as the Peutinger Table (Marin, 2018; Totten, 2022), have gestured towards the close links
84 between settlement on the lagoon and salt production.

85 In order to fill ~~this~~ gap, this paper presents for the first time ~~the~~ sedimentological,
86 palynological and micropalaeontological results of continuously drilled boreholes collected
87 within the area of the "Capitanata" at the southern margin of the coastal plain. ~~This study~~
88 ~~aims to shed light on the processes that have shaped the coastal dynamics and the relative~~
89 ~~influence of the natural and anthropic forcing factors that have driven the evolution of the~~
90 ~~coastal plain during the Holocene, so that future studies could begin to link the~~
91 ~~palaeoenvironmental results to the archaeological data,~~

92 2. Study area

93 The so-called "Capitanata" (Fig. 1) covers an area of 440.459 hectares. It lies within the
94 southern margin of the Tavoliere coastal plain, bordered on the north by the Gargano
95 Promontory (northern part of the Apulian foreland), on the west by the southern Apennines
96 chain (known as *Subappennino Dauno*), on the east by the Gulf of Manfredonia (Adriatic Sea),
97 and on the south by the Ofanto River watershed. Four major rivers flow into the Gulf of
98 Manfredonia, from north to south: the Candelaro River, the Cervaro River, the Carapelle
99 River, and the Ofanto River. The latter is the main watercourse of the area and the main
100 geomorphological control feature of the coastline dynamics (Simeoni, 1992; Caldara, 1996;
101 Spagnoli et al., 2008; De Santis et al., 2018).

102 Due to the abundance of water, the flat morphology, and the altitude, often below sea-level,
103 the area was routinely affected by seasonal flooding, resulting in ~~unhealthy~~ conditions for
104 the population. For these reasons, the area was the subject of an extensive infrastructural
105 land reclamation project which began in the 1920s and drained the wetlands through
106 embankments and direct channelling (e.g. Marana Castello, C.le Carapellotto, C.le Regina
107 and F.so della Pila, Fig. 1). Moreover, the Tavoliere coastal plain underwent various land-
108 tenure, agronomic, and hydraulic re-organisation phases, leading up to the agrarian reform
109 of 1951 and the consequent completion of a large-scale irrigation infrastructure, which is
110 still the main feature of the area (Ciccone, 1984; Russo, 1985).

111 The climate of the study area is semi-arid, with mean annual precipitation below 500
112 mm/year (Battista et al., 1993). The scarcity of humid air masses coming from the
113 surrounding mountains reduces seasonal variability and results in dry conditions in
114 summer. The natural vegetation of the coastal plain and the southern slopes of the Gargano
115 Promontory consists of steppic plants with patches of Mediterranean elements (Biscotti,
116 2001). Nonetheless, agricultural activities have shaped the landscape since prehistoric times
117 (Barker et al., 1987). In contrast, dense mixed forests of oak, beech, and conifer woods are
118 widespread on the headland (Biscotti, 2001).

119 2.1. Geological background

120 Structurally, the area belongs to the Bradanic foredeep, which opened at the beginning of
121 the Lower Pliocene and gradually filled throughout the Late Quaternary (Tropeano et al.,

122 2002). At the same time, the area underwent phases of subsidence and discontinuous
123 tectonic uplift (Doglioni et al., 1994; 1996), with the onset at the end of the Early Pleistocene.
124 Thus, the vertical sedimentary succession shows a general polycycle transgressive-
125 regressive trend from marine to continental depositional environments.

126 The first sedimentary cycle occurred between the Middle Pliocene and the Early Pleistocene,
127 overlaying the Mesozoic limestones basement of the Apulian foreland, which forms a
128 system from west to east in the Gargano headland (Pieri et al., 1996; 1997). The transgressive
129 units belong to the "Bradanic cycle" (De Santis et al., 2010 and reference therein) and consist
130 of shallow-marine carbonate deposits passing conformably upward to silty-clayey
131 hemipelagic deposits (Fig. 1).

132 The second sedimentary cycle, unconformably overlaying the Plio-Pleistocene carbonate
133 deposits, occurred during the Middle Pleistocene and continued throughout the Holocene
134 due to the uplift of the Apulian foreland (Pieri et al., 1996; 1997; Patacca and Scandone, 2001;
135 Mastronuzzi and Sansò, 2002b) and the glacio-eustatic sea-level changes (Mastronuzzi et al.,
136 2011; Maselli and Trincardi, 2013; Maselli et al., 2014). These processes resulted in several
137 marine and continental terraces (De Santis et al., 2010), which are also recognised in many
138 areas of the Bradanic foredeep (Boenzi et al., 1991; Gallicchio et al., 2014; De Santis et al.,
139 2021). Thus, the sedimentary sequence, going unconformably from the oldest to the
140 youngest deposits according to their progressive elevation from sea-level, consists of
141 shallow marine and infralittoral sandy deposits, continental conglomerates deposits,
142 alluvial sandy-gravelly deposits, and recent and present-day alluvial plain deposits (De
143 Santis et al., 2010, Fig. 1).

144 During the Holocene, climate amelioration and sea-level rise (Dini et al., 2000; Primavera et
145 al., 2011; De Santis and Caldara, 2015; Vacchi et al., 2016; De Santis et al., 2020) resulted in
146 the formation of a lagoon within the coastal plain, dammed seaward by a system of coastal
147 dune belts (Caldara and Pennetta, 1993b; Mastronuzzi and Sansò, 2002a), which stretched
148 ca. 40 km at its maximum extension, from the foothill of the Gargano Promontory to the
149 delta of the Ofanto River (Caldara and Pennetta, 1990; 1992; Caldara et al., 2002). Whilst the
150 chronology for assessing the palaeo-lagoon is still uncertain, archaeological data suggest
151 that wetlands were most likely already present during the Early Neolithic (Di Rita et al.,
152 2011 and references therein). Since the Northgrippian (Walker et al., 2018), the coastal

153 lagoon has undergone several changes, both in terms of dimension and environment
154 (Caldara and Pennetta, 1993a; Boenzi et al., 2001; 2006; Caldara et al., 2002; Di Rita, 2013),
155 up to the recent definitive land reclamation (Cicccone, 1984; Russo, 1985).

156 2.2. Archaeological background

157 The Tavoliere coastal plain, like many other areas of the northern coast of Apulia, has been
158 densely populated since the Neolithic period (6.5 ka-3.7 ka BCE, Hamilton and Whitehouse,
159 2021). The inhabitants practised agriculture and livestock breeding, and exploited the
160 locally available natural resources (Tafari et al., 2014; Muntoni et al., 2022). Between the Late
161 and Final Neolithic (5th and early 4th millennium BCE), drier climatic conditions (Caldara
162 and Pennetta, 1993b; Boenzi et al., 2001; Fiorentino et al., 2013) are considered the main
163 reason for the sudden abandonment and massive depopulation of the coastal plain
164 (Whitehouse, 2014). In addition, this drought induced people living in the Tavoliere to adopt
165 a more pastoral type of farming (Whitehouse, 2014).

166 Re-colonisation of the coastal area most likely began during the Copper Age (4th-3rd
167 millennium BCE) and intensified during the Bronze Age (early 2nd millennium BCE - 12th
168 cent. BCE), when numerous sites ~~have been documented~~ along the northern Adriatic coast
169 and at key inland locations (Cazzella et al., 2017). However, most of these settlements were
170 short-term small villages devoted to agro-pastoral activities or salt exploitation. In the
171 Tavoliere coastal plain, however, the most important archaeological evidence is the fortified
172 settlement of Coppa Navigata, located south of the Gargano Promontory (Fig. 1). This
173 settlement was continuously inhabited until the Early Iron Age (18th-8th cent. BCE) and
174 practised craft and exchange activities (Cazzella et al., 2012), eventually shifting towards
175 agricultural production and subsistence strategies (Primavera et al., 2017).

176 During the Iron Age, archaeological and historical data (Goffredo, 2014 and references
177 therein) indicate that the Tavoliere coastal plain was intensively colonised by Daunian
178 settlements. These settlements developed over time into new central places, the most
179 important of those being *Arpi* (off-map), *Cupola-Beccarini* (*Daunian Sipontum* in the
180 figures) and *Salpia Vetus* (Fig. 1, Marin, 1973). During the 5th-4th cent. BCE, these indigenous
181 settlements developed into proto-urban centres with strong, local, Hellenised aristocracies,

182 whose wealth was based on land-tenure, breeding, production and trade of cereals
183 (Buglione et al., 2016).

184 According to the chronicles of Vitruvius, between the 3rd and 1st cent. BCE, the marshland
185 conditions surrounding the city of *Salpia Vetus* became insalubrious. As a result, the
186 population was forced to move away from the lagoon and founded a new urban centre
187 called *Salapia*, about 6 km from the abandoned *Salpia Vetus* and closer to the coastline (De
188 Venuto et al., 2022). Archaeological excavations carried out in different parts of the
189 settlement have highlighted the main frequentation sequences from the 1st cent. CE to the
190 8th cent. CE (De Venuto et al., 2022). Moreover, archaeological findings of pier-like structures
191 on the coast of Torre Pietra suggest that the settlement of *Salapia* was connected to the sea
192 (Volpe, 1990; Cocchi et al., 2012).

193 Over the 9th cent. CE (Early Middle Ages), the settlement of *Salapia* was largely abandoned,
194 although human occupation probably continued within the ruins of some sectors of the city.
195 The re-foundation of the settlement and its community was not completed until the 11th
196 cent. CE (Late Middle Ages), when *Salpi* (no longer *Salapia*) regained its status as a city
197 (Goffredo, 2021). The new medieval settlement was reorganised at a significantly higher
198 elevation than the surrounding countryside, and enclosed by a deep moat, probably served
199 for defensive and drainage purposes (Goffredo, 2021).

200 2.3. Palaeoenvironmental background

201 The diachronic palaeoenvironmental reconstruction of the wetlands in the Tavoliere coastal
202 was initially based on the study of some agricultural trenches and cores drilled in the
203 northern area for water research (Boenzi et al., 2001). During the Early Neolithic, the lagoon
204 was characterised by euryhaline and eurythermal molluscs living in brackish water or
205 muddy sands of sheltered zones. After 6.3 ka BP, the lagoon evolved into a *sabkha* (Caldara
206 and Pennetta, 1993b; Boenzi et al., 2001), a saline sand/mud flat area where evaporite
207 minerals (gypsum) accumulated under arid conditions are associated with desertification
208 processes. According to Caldara et al. (2004), this event led to the abandonment of coastal
209 settlements of the Tavoliere at the end of the Neolithic.

210 New systematic coring activities near the archaeological site of Coppa Nevigata (Caldara
211 and Simone, 2005; 2012; Caldara et al., 2004; Di Rita et al., 2011) provided detailed

212 information on the evolution of wetlands and the surrounding vegetation in relation to the
213 human occupation of this portion of the coastal plain. A brackish lagoon
214 with *Hydrobiidae* spp. and *Cerastoderma glaucum* was identified between 3600 and 3090 BP,
215 followed by alternating terrestrial, wetland and salt marsh phases up to 370 ± 50 BP (Caldara
216 et al., 2004). As no evidence of sea-level fluctuations was found towards the middle of the
217 basin, such deposition of terrestrial/marshy sediments was interpreted as aggradation of
218 the coastline due to human colonisation of the lagoon shore between the Neolithic and the
219 Iron Age (Caldara and Simone, 2005). Away from the settlement, a brackish wet
220 environment was established before 6340 BP with local changes caused by salinity
221 fluctuations leading to a progressive transformation of the semi-closed lagoon into a coastal
222 lake until 3230 BP (Di Rita et al., 2011).

223 After an erosive episode around 370 ± 50 BP, a seasonal freshwater marsh formed around
224 the end of the Middle Ages, which evolved into a terrestrial environment until the historical
225 reclamation. Locally, saltmarsh vegetation still existed towards the sea, whereas inland, a
226 deforested landscape consisting mainly of pastures and cultivated fields was widespread
227 (Caldara et al., 2004; Caroli and Caldara, 2007; Di Rita et al., 2011).

228 **3. Materials and methods**

229 Analyses were carried out on a total of 10 drilled boreholes (Fig. 2) obtained during two
230 coring campaigns in 2017 (cores labelled SAL, Tab. 1) and 2019 (cores labelled SAM, Tab. 1).
231 The location of the cores followed a geomorphological survey and mapping of the area, also
232 taking into account the two archaeological sites of *Salpia Vetus* and *Salapia-Salpi*. The first
233 two coring campaigns were performed using a drilling machine equipped with a hydraulic
234 piston, a 1 m-long cylindrical corer, and a 101 mm-diameter cutting shoe (max. depth of 16
235 m). For the 2019 coring campaign, a gasoline-powered percussion hammer was used (max.
236 depth of 9 m). Both drilling systems and sedimentological characteristics allowed for ca.
237 90% recovery of the whole sedimentary sequence. The cores were studied and sampled in
238 the laboratories of IGAG-CNR and INGV (Rome, Italy).

239 Calibrated AMS ^{14}C ages were obtained from 21 selected charcoal, ostracod shells, and
240 organic sediments. Samples were processed by Beta Analytic Radiocarbon Dating (Miami,
241 USA), using pre-treatment of acid washes and acid-alkali-acid protocols for organic

242 sediments and sonication in de-ionised water for shells. Calibrated dates were calculated
243 using the BetaCal4.20 protocol, based on the IntCal20 calibration curve database (Reimer et
244 al., 2020) and the high probability density range (Bronk Ramsey, 2009). Dating performed
245 on ostracod shells used Siani et al. (2000) as reference for the MARINE20 curve selection.

246 The sedimentary sequence was described following the facies analysis method (Miall, 1985;
247 2010), taking into account texture, colour, fabric and sedimentary structures, biological
248 remains and pedological features. Sediment colour has been determined with the Munsell
249 Soil Colour Charts under moist conditions.

250 SAM and SAL cores were sampled for a ~~total of 200 micropaleontological samples~~. All
251 samples were processed following the standard procedure of drying, disaggregation in
252 ~~diluted hydrogen~~ peroxide solution (20%), washing in 1.25 mm and 0.63 mm mesh sieves
253 and drying in an oven at 50°C. Each dried and sieved sample was observed using a
254 stereomicroscope (X14-150) to identify ostracoda, charophytes, foraminifera (planktic and
255 benthic) and other biogenic remains. For the ostracod analysis, Ostracods Ecological Groups
256 (OEG) were used, following Mazzini et al. (2017). The OEG enables standardising species
257 by their ecological tolerance (SM: Shallow Marine, BM: Brackish to lagoonal Marine, EU:
258 Euryhaline and FLB: Freshwater to Low Brackish) and reduces to 4 quantitative variables
259 (% of each OEG) the biological information brought by the fossil assemblages of ostracods.

260 The grain size analysis has been performed in SAM9, on 15 samples, using a fraction of 30
261 g of dry sediment. Coarse fraction (>2 mm), sand (2 mm), silt (63 mm) and clays fraction
262 (<63 mm) were differentiated through weighing sieve residue.

263 Palynological analysis was conducted on 58 sediment samples collected from SAL2, SAL3,
264 and SAM9 cores. For each sample, 1.70 to 2.70 g of dry sediment was chemically processed
265 for removal of detrital matter, following Fægri and Iversen (1989) method, with the
266 alternating treatment of HCl (37%), HF (40%) and hot NaOH (10%). Following Stockmarr
267 (1971), tablets containing a known amount of *Lycopodium* spores were added to estimate
268 concentrations of pollen, spores, NPPs (Non-Pollen Palynomorphs) and microcharcoals.
269 The identification of pollen morphology is based on pollen atlases and taxonomic keys
270 (Fægri and Iversen, 1989; Moore et al., 1991; Reille, 1992; 1995; 1998; Beug, 2004) and
271 reference pollen collections. *Quercus* species are grouped as described by Smit (1973),

272 whereas pollen grains of cereals have been distinguished within the Poaceae family
273 following Andersen (1979). Cichorieae corresponds to the only European tribe of Asteraceae
274 with fenestrate pollen grains belonging to the subfamily Cichorioideae (Florenzano et al.,
275 2015). The pollen percentages have been calculated on the basic pollen sum, which includes
276 all the terrestrial spermatophytes; percentages of macrophytes, ferns, green algae,
277 cyanobacteria, fungi, and *Pseudoschizaea* have been calculated as the sums of terrestrial
278 spermatophytes plus, in turn, each group of considered palynomorphs (Berglund and
279 Ralska-Jasiewiczowa, 1986). The concentration values have been calculated per weight unit
280 of dried sediment (pollen grains and NPP remains /g). The influx values have been obtained
281 from the concentration values based on the sedimentation rates inferred from the age-depth
282 model (grains/cm² year; Berglund and Ralska-Jasiewiczowa, 1986). Pollen influx (i.e., the
283 amount of pollen grains incorporated annually per unit of sediment) is an estimation of the
284 plant biomass. The pollen diagrams have been plotted against depths using the TILIA
285 program (Grimm, 1992). All Arboreal Pollen (AP) and Non-Arboreal Pollen (NAP) taxa with
286 values of the basic pollen sum higher than 2 % have been considered in the CONISS cluster
287 analysis, which supported the pollen zonation (Grimm, 1992). Charcoal particles have been
288 identified and counted from pollen slides in order to evaluate the fire impact on past
289 landscape. Following Sadori and Giardini (2007) and Whitlock (2010) the fragments have
290 been sorted in three dimensional classes, which represent regional fire (10-50 µm), fire
291 occurred at landscape/regional scale (50-125 µm), and local fire (>125 µm). Data are
292 presented as concentration values (charcoals/g).

293 **4. Results**

294 4.1. Chronology

295 The relative scarcity of datable material did not allow for obtaining a very consistent
296 chronological sequence for all available cores, except for the SAM9 core (Tab. 2). In addition,
297 5 dates have been rejected due to chronological inversion or exceptionally ancient age, most
298 likely due to surface runoff processes. Available dates show a good chronological coherence,
299 with an interval spanning from the Late Northgrippian (6210-6001 cal BP, SAM9-724b, Tab.
300 2) to the Late Meghalayan (231-124 cal BP, SAL3_260, Tab. 2). It is worth noting that dates
301 obtained at the base of SAM9 (from SAM9_724a to SAM9_730b) also display a chronological
302 inversion. However, the short distance that elapses from one dating to another (approx. 6

303 cm) and the smallness of the chronological gap make it possible to consider them all valid.
304 Moreover, the age-depth model is based on 3 AMS 14C ages as reported in Tab. 2. It is used
305 for all data from the SAM9 core presented in this study

306 4.2. Facies Analysis

307 The description of the sedimentary facies observed in all cores allowed the identification of
308 5 main sedimentary facies associations grouped into Alluvial facies (AF), Swamp-Marshy
309 facies (SMF), and Lagoon-Brackish facies (LBF). Additionally, a series of cm-thick tephra
310 layers have been recognised in SAL1 and SAL3 cores. They consist mainly of grey (7.5YR
311 6/1) fine- and medium-grained ash with common pyroclastic material made of irregular
312 pumice fragments. However, the tephra layers resulted in being altered and weathered to
313 varying degrees, making them unsuitable for chemical and microprobe analysis (Giaccio, B.
314 personal comment).

315 4.2.1. Alluvial facies (AF)

316 AF1 – this facies consists of greyish brown (10YR 5/2) to brown (10YR 4/3) silts with fine-
317 grained sands (Fig. 3abc). Locally, scarce fine gravels and occasional subangular cm-sized
318 pebbles are present. The facies is massive and occasionally interbedded with few cm-thick
319 (3-5 cm on average) fine-grained sand layers. The colour variation is due to the varying
320 proportion of sands and silts. Fine rootlets are occasionally present, although neither
321 organic matter nor charred material have been observed. Common redox Fe-Mn mm-sized
322 nodules (0.2 mm on average), rare mottles, and abundant secondary carbonate precipitation
323 in mm- to cm-sized (0.3 mm to 1.5 cm on average) nodules are present. Stratigraphy
324 boundaries are mainly sharp and clear. The sedimentary features and architectural elements
325 are consistent with distal partially- to well-drained or partially flooded floodplains under
326 low-energy conditions, although the presence of gravel and pebbles indicates short-term
327 high-energy events. The interbedded thin sandy layers suggest the occurrence of sand
328 sheets or sand splays due to the nearby presence of channels. The presence of rootlets and
329 the development of secondary carbonate and redox features point to weakly pedogenetic
330 post-depositional modification, thus indicating rapid episodes of sub-aerial exposure under
331 well-drained conditions.

332 AF2 – this facies consists of alternating cm-thick brown-greyish brown (7.5YR 4/3 to 10YR
333 5/2) to dark yellowish-brown (10YR 4/4) massive silty-sand facies with fine gravel and rare
334 pebbles and dark brown (10YR 3/3) moderately laminated silty-clayey facies (Fig. 3b).
335 Locally, the sandy to silty facies show fining- upward trend with sharp lower boundaries,
336 locally erosive where the pebbles and gravels are present. Scarce redox Fe-Mn mm-sized
337 nodules (0.2 mm on average) and common secondary carbonate precipitation in mm-sized
338 (0.5 mm on average) nodules are also present. Locally, the sand bodies are red-coloured
339 (2.5YR 7/3 to 2.5YR 5/6). Although no organic matter has been observed, scattered mm-
340 sized (0.1 mm on average) charcoal fragments are present. The overall facies association
341 reflects a channel-related deposit. The alternation between silty-sands and silty-clays facies
342 is consistent with rhythmical depositional sub-environments related to natural levees. The
343 gradual channel filling, with decreasing bedload energy, is attested by the fining-upward
344 trends from gravel to sandy-silt to silty-clayey, whilst bodies with erosive lower boundaries
345 are most probably related to channel migrations or crevasse channels within which the
346 bedload was conveyed. Pedogenic features testify to a short-term subaerial exposure
347 determined by the topographically elevated areas formed by the natural levees and crevasse
348 splays.

349 AF3 – this facies is made of brown (7.5YR 4/3) coarse-grained sand with common fine- to
350 coarse gravel and pebbles (Fig. 3c), the latter with smooth surfaces. The facies shows a local
351 fining-upward trend, where pebbles are found above erosive lower boundaries. Locally, the
352 succession is capped by 1 cm- thick dark brown (7.5YR 3/3) clayey-silt layers, with sharp or
353 transitional boundaries when located at the top of the succession. The overall sedimentary
354 features are typical features of fluvial-channel deposits. The sharp boundaries between
355 sands and silty layers likely indicate an abrupt abandonment of the channel, whereas the
356 gradual transitions may reflect a gradual filling of the channel.

357 4.2.2. Swamp – Marshy facies (SMF)

358 SMF1 – this facies consists of dark greenish-grey (5GY 4/1) to dark grey (7.5YR 4/1) massive
359 clay and silty-clay, with local occurrence of cm-thick greyish brown (10YR 5/2) massive fine
360 sand beds with abundant unidentifiable fine shell fragments at the base (Fig. 3d). Occasional
361 mm-sized charcoal or charred fragments are also found. Concentrations of organic matter
362 with very fine rootlets infrequently occur in a few cm-thick peaty layers with gradual lower

363 boundaries and clear upper boundaries, along with local reddish-yellow (7.5YR 6/8)
364 mottles of Fe-Mn oxides. The overall facies indicates a very low-energy depositional
365 environment consistent with swampy-marshy areas such as ponds or coastal lakes that were
366 occasionally subjected to rapid sub-aerial processes, as indicated by Fe-Mn oxides mottles.
367 The sporadic presence of organic matter and thin peaty layers suggests these as mostly non-
368 vegetated or occasionally weakly vegetated environments, whilst sandy layers reflect
369 occasional short high-energy ingressions of river floods from adjacent fluvial channels.


370 4.2.3. Lagoon – Brackish facies (LBF)

371 LBF1 – this facies consists of monotonous greenish-grey (5GY 6/1) massive clay (Fig. 3e)
372 with scattered rare marine shell fragments of *Cerastoderma*. Lower and upper boundaries
373 are mostly gradual. The homogeneous sedimentary features and the overall absence of
374 architectural elements suggest deposition from suspension under low-energy conditions.
375 The light grey colour is possibly related to the almost absence of organic matter, whilst the
376 presence of marine shell fragments is indicative of reworking by storms within shallow to
377 deep lagoon or brackish environments partially connected to the open sea.

378 LBF2 – this facies consists of very dark grey (10YR 3/1) to very dark brown (10YR 2/2)
379 massive silts with clay and very scarce sand, with abundant enrichment of fibrous organic
380 matter, charred or poorly decomposed plant fragments (Fig. 3e). The distinctive
381 sedimentological features indicate for this facies association a low-energy depositional
382 setting, rich in wood vegetation, in which organic material was able to accumulate due to
383 the decreasing energy. The overall facies is consistent with a marginal-shallow and well-
384 vegetated lagoonal environment.

385 4.3. Micropalaeontological analyses

386 ~~Micropalaeontological analyses were carried out on the cores and the most suitable~~
387 ~~sediments (clays to fine-grained sands).~~ Although ostracods were the most abundant group,
388 dominating the total microfauna, their occurrence is scattered in SAL1 and SAL2 cores and
389 in the SAM cores. SAL3 was totally barren. In general, all the ostracod species observed in
390 the cores are referable to the OEGs euryhaline and freshwater to low brackish, whereas the
391 marine component lacks completely. In SAL1 and SAL2, in the AF1, AF2 and AF3 facies,
392 only the OEG freshwater occurs, with species typical of springs or waters connected to

393 springs (*Cypria ophtalmica*, *Ilyocypris bradyi*, *Herpetocypris brevicaudata*, *Prionocypris zenkeri*).
394 In SAM1, SAM5, SAM6, SAM7 and SAM8, in the SMF1 facies, *Candona* gr. *neglecta*,
395 *Pseudocandona* gr. *marchica* and *Limnocythere inopinata* occur, all species tolerating a wide
396 range of environmental conditions. *Characeae* gyrogonites are also present in some samples,
397 indicating relatively shallow depths and clear waters. The foraminifera observed were
398 most  displaced or reworked from older sediments.

399 In SAM9, ostracods are abundant and occur within the whole cored sedimentary sequence.
400 A total of 7 ostracod species were identified: *Cyprideis torosa*, *Candona* gr. *neglecta*,
401 *Heterocypris salina*, *Ilyocypris bradyi*, *Eucypris virens*, *Limnocythere inopinata*, *Cypridopsis vidua*.
402 *C. torosa* only occurs with smooth shells. The densities of the identified ostracod species for
403 each sample are shown in Fig. 4, together with the occurrence of the two foraminifera
404 species *Ammonia tepida* and *Haynesina germanica*, diatoms, *Characeae*, fish remains and
405 ephippia *Daphnia*-type. Through the correlation of all these proxies, four different zones
406 were identified:

407 MZ1 (730-613cm; 5348-4198 BP) – the lowermost part of the core is characterised by the
408 occurrence of *Cerastoderma* cockles, abundant *Cyprideis torosa*, and scattered occurrence of
409 *Cypridopsis vidua* and charophyte gyrogonites. *Ammonia tepida* and *Haynesina germanica* are
410 alternately represented.

411 MZ2 (590 -480cm; 3970-3115 BP) – *I. bradyi* and *E. virens* become the dominant species,
412 followed by *C. torosa* and *C. vidua*. *A. tepida* and *H. germanica* are poorly represented except
413 in the uppermost samples.

414 MZ3 (465-259 cm; 3075-2489 BP) – this is the most diversified interval, where all ostracod
415 species are represented with frequencies lowering towards the top. Charophyte gyrogonites
416 are abundant, and diatoms also occur. Ephippia *Daphnia*-type is observed only in the
417 uppermost samples. At around 350 cm, *A. tepida* and *H. germanica* disappear.

418 MZ4 (239-52 cm; 2286-446 BP) – the uppermost zone is characterised by low ostracod
419 frequencies (*L. inopinata*, *E. virens* and scarce *C. torosa*) and few reworked and displaced
420 foraminifera. Fish remains (pharyngeal teeth of Cyprinids) are abundant.

421 4.4. Pollen analysis

422 Due to the scarcity and bad preservation of pollen grains in SAL2 and SAL3 cores, only
423 results from the 26 samples of SAM9 core are described. The mean pollen count per sample
424 is 253. A total of 76 terrestrial pollen taxa have been identified, including 33 arboreal, 43
425 herbaceous plants plus 13 taxa of water plants and NPPs. AP prevails only in the lowermost
426 two levels, up to 58 % of the total pollen sum. Pollen concentrations range from 1232 (at 196
427 cm - 1870 BP) to 59,193 (at 700 cm - 5050 BP) pollen grains/g. The percentage and
428 concentration values of selected taxa are shown in Fig. 5 and Fig. 6.

429 Four pollen assemblage zones (PAZ) are described from bottom to top. Pollen zonation is
430 based on CONISS cluster analysis and visual inspection.

431 4.4.1. PAZ 1 (720-619 cm; 5250-4260 BP)

432 At the bottom of the sequence AP values decrease from 58% to 26%. The total pollen
433 concentration reduces from 59,193 to 10,995 pollen grains/g. *Quercus robur* type (max. 20%)
434 and *Quercus cerris* type (max. 6 %) in association with *Ostrya/Carpinus orientalis* (max. 7%)
435 prevail between mesophilous taxa. ~~Mediterranean~~ vegetation is mainly dominated
436 by *Juniperus* (max. 12%) and *Quercus ilex* type (max. 8%). *Alnus* (max. 8%) ~~well~~ represents
437 riverine trees. Among herbs, Poaceae (max. 23%) and Amaranthaceae (max. 35%) prevail
438 with an opposite trend of decrease (former) and increase (latter). Cereals pollen is poorly
439 but significantly present (max. 2%) and is accompanied by pollen of *Plantago* undiff. (max.
440 4%), *P. lanceolata* type (max. 3%), *Urtica* (max. 5%). Charcoal concentrations of the 10-50 µm
441 dimensional class vary from 10,321 to 202 charcoals/g.

442 4.4.2. PAZ 2 (602-452 cm; 4090-3040 BP)

443 AP (max. 22%) progressively decreases, with a minimum of 2 % at 452 cm. All the arboreal
444 taxa, apart from *Abies* (max. 1 %) strongly reduce. *Olea* is absent, whereas *Juglans* (max. 1%)
445 appears in this zone at ca. 3210 years BP. Herbs are predominant and almost exclusively
446 dominated by Amaranthaceae (max. 90%), as also evidenced by concentration values where
447 the peak of Amaranthaceae (40,425 charcoals/g) correspond to the increase of total pollen
448 concentration at ca. 3040 BP. A special mention is due to *Urtica* (max. 8%), increasing
449 through the zone. The highest peak of charcoal concentration (19,815 charcoals/g) is
450 recorded at ca. 3210 BP when the >125 µm dimensional class is attested. The

451 overrepresentation of local halophilous non arboreal vegetation probably emphasizes the
452 forest opening.

453 4.4.3. PAZ 3 (400-269 cm; 2900-2550 BP)

454 ~~The~~ pollen zone shows important differences and is characterised by a low amount of AP
455 (max. 30%). The total pollen concentration is still dominated by herbs (Amaranthaceae:
456 19,090 pollen grains/g at ca. 2740 BP). First a mesophilous vegetation, with *Quercus*
457 *robur* type (max. 8%), *Quercus cerris* type (max. 4%), *Ostrya/Carpinus orientalis* (max. 3%),
458 *Carpinus betulus* and *Fraxinus excelsior* type (max. 1% and 3%, respectively) is present and
459 accompanied by ferns; then, freshwater riverine vegetation expands, first with a peak of
460 *Typha angustifolia* type (max. 22%) and *Potamogeton* (max. 3%), then with riparian trees such
461 as *Alnus* (max. 11%) and *Populus* (max. 1%). Worthy of mention is the presence of green
462 algae (i.e. Zygnemataceae, max. 4% and *Botryococcus*, max. 3%) in the uppermost part of the
463 zone. ~~The Mediterranean shrubland increases at the end of the zone~~ when the record shows
464 a significant peak of *Juniperus* (max. 19%). Apart from Amaranthaceae (max. 74%), which
465 continue to dominate all over this zone, Cyperaceae (max. 15%) and Liliaceae (max. 4%) are
466 the main NAP taxa. At the same time, herbs from dry environments, such as Asteroideae
467 (max. 10%), start to expand. Moreover, a two-folded expansion of *Gloeotrichia*, a
468 Cyanobacteria genus, is recorded at ca. 2740 BP both in percentage (max 30 %) and
469 concentration (12,666 NPP remains/g) values. Concentration values of charcoals are low
470 (max. 1369 charcoals/g).

471 4.4.4. PAZ 4 (250-54 cm; 2400-470 BP)

472 AP oscillates from 0% to 23% in this uppermost pollen zone. Mediterranean taxa from
473 shrublands increase (i.e. *Ephedra*, max. 6%; *Pistacia*, max. 5%; Ericaceae, max.
474 1%). *Olea* (max. 4%) also expands in this zone, seeming to correlate with the increase
475 of *Juglans* (max. 2%). Cichorieae (max. 72%) from dry and pastured environments suddenly
476 substitute Amaranthaceae (max. 14%) as predominant herbs and increase exponentially in
477 this zone as clearly attested by concentration values (12,237 pollen grains/g in the
478 uppermost level). The *Hordeum* group (max. 8%) increases among cereals,
479 *Avena/Triticum* (max. 1%) and *Secale* (max. 1%) show their first appearance in the record.
480 Weedy herbs are represented by *Centaurea* (max. 2%) whilst Apiaceae (max. 5%) and

481 Brassicaceae (max. 13%) also increase. The highest values of ferns (i.e. monolete spores, max.
482 14% and trilete spores, max. 6%), green algae (i.e. Zygnemataceae, max. 11%
483 and *Botryococcus*, max. 7%), fungi (i.e. *Glomus*, max. 7%), and *Pseudoschizaea* (max. 8%) of the
484 record are found. A significant peak of charcoal concentration (8369 charcoals/g) is attested
485 at ca. 1460 BP when all the dimensional classes are represented.

486 5. Palaeoenvironmental reconstruction

487 The stratigraphic data from the new drilled cores of the "Capitanata" show the interplay
488 between coarse-grained alluvial facies and silty-sandy swamp/marshy facies in controlling
489 the evolution of the southern margin of the Salpi lagoon (Fig. 7), whilst lagoonal facies are
490 only observed at the bottom of the sedimentary sequence of the SAM9 core (Fig. 7). On the
491 one hand, one of the most striking features of the sedimentary sequence of the cores is the
492 poor chronological resolution due to the average coarse grain size (silty sands to coarse
493 sands), the general lack of organic matter, and the poor preservation of pollen grains. On
494 the other hand, the sedimentary sequence of the SAM9 core has resulted in a reliable age-
495 depth model, based on a set of consistent ¹⁴C dates. Thus, facies analysis, coupled with
496 micropalaeontological and pollen data, indicates that the coastal lagoon in the area of the
497 "Capitanata" gradually shifted from a transitional marine-brackish environment into a more
498 sheltered environment, influenced by freshwater inputs, leading to the complete emersion
499 due to the alluvial plain progradation. This regressive sequence is commonly recorded in
500 many Mediterranean coastal plains (Lakhdar et al., 2004; Sacchi et al., 2014; Carmona et al.,
501 2016; López-Belzunce et al., 2020).

502 5.1. Late Northgrippian (5.2 ka–4.2 ka BP)

503 Between ca. 6.2 ka and 3.1 ka cal BP, sedimentary facies from the SAM9 core indicate that
504 the southern portion of coastal plain was occupied by a semi-open coastal lagoon that was
505 partially connected to the sea. The dominance of the euryhaline species *C. torosa*, which has
506 a wide tolerance to hydrological changes such as temperature and salinity, confirms the
507 occurrence of a lagoonal environment, whilst the occurrence of the foraminifera *A.*
508 *tepida* and *H. germanica* points to an aquatic environment characterised by fluctuating
509 temperatures and food sources (Fig. 8, Lintner et al., 2020). The lack of chronology for the
510 inner areas of the coastal plain (cores SAL1, SAL2 and SAM1) prevents further hypotheses.

511 However, the presence of four tephra layers within the floodplain environments in the SAL1
512 core (Fig. 7), although too altered to be identified, could be ascribed between the fallout
513 phase of the Plinian 3.7 ka BP Avellino eruption of Vesuvius and the AP3 phreato-Plinian
514 2.8 ka BP Somma-Vesuvius eruption (Andronico and Cioni, 2002; Calanchi and Dinelli,
515 2008; Santacroce et al., 2008), as also demonstrated by Caldara and Simone (2005) in the
516 Tavoliere coastal plain. If such is the case, these tephra layers could be considered as
517 a *terminus ante-quem* for the progradation of floodplain environments in the innermost area
518 of the coastal plain. In fact, considering the stratigraphic depth at which the lagoonal
519 environments are observed, Fig. 7 clearly shows that the innermost part of the coastal area
520 was already deactivated and characterised by floodplain environments (SAL1 core) and
521 marshlands (cores SAL2 and SAM1). The emergence of these environments was likely the
522 result of the distribution of the sedimentary load from the former palaeodrainage of the
523 Carapelle River prior to the anthropic drainage regulation, which bypassed the threshold of
524 the Upper Pleistocene alluvial deposit (Fig. 9a).

525 The dominance of alluvial environments is also observed in cores SAM4 and SAL3 (Fig. 7),
526 collected close to the archaeological site of *Salapia-Salpi* and at the top of the Upper
527 Pleistocene alluvial deposits. Thus, these cores confirm that this part of the coastal plain was
528 already stable and not affected by lagoonal or marshland environments during the
529 Holocene.

530 The vegetation of the lagoon also testifies to the widespread presence of freshwater
531 elements. In fact, among the riparian trees, *Alnus* (alder) shows high values from the
532 sequence bottom to ca. 4200 cal BP. Poaceae pollen could refer to *Phragmites* (reeds),
533 although this family also includes grasses of dry meadows, whose distribution in the
534 surrounding drylands is evidenced by pollen of *Plantago lanceolata* type (ribwort plantain,
535 Fig. 6). Other species of *Plantago* are halophytes, associated with brackish environments, as
536 attested today in the Apulian region (Marchiori et al., 1998). However, from 4.8 ka BP the
537 pollen concentrations drop, whilst halophytic herbs (Amaranthaceae) exponentially
538 expanded (Fig. 8). The growth of saltmarsh vegetation indicates an increase in salinity,
539 possibly related to the progressive shallowing of waters and closure of the lagoon.

540 At around 5 ka cal BP and 4.1 ka cal BP (Fig. 5), the palynological record shows two peaks
541 of pollen of the pioneer shrubs *Juniperus* (juniper), indicating the formation of sand barriers

542 seaward. This differs from the circumstances in the Lago Salso, in which an increase of
543 *Juniperus* is only evident at ~4 ka BP (Di Rita et al., 2011). Thus, this evidence confirms the
544 northward progradation of the dune coastal barriers and the progressive closure of the
545 southern portion of the lagoon, in contrast to the picture painted by Caldara and Simone
546 (2005) and Di Rita et al. (2011) in the northern sector, who report that the lagoon was open
547 to the sea (*Hydrobiidae* spp. and *Cerastoderma* lagoon) between 6.3 ka and 3.2 ka cal BP. The
548 overall evidence is consistent with the marine direction of sediment transport reconstructed
549 by De Santis and Caldara (2015) and De Santis et al. (2020) before the Holocene climatic
550 transition (5.5 ka–4.5 ka cal BP). The anticyclonic gyre is also responsible for the distribution
551 of Ofanto River sediments toward north and northwest and into the central area of the Gulf
552 of Manfredonia (Spagnoli et al., 2008). The gradual development of sand barriers favoured
553 the progressive isolation of the brackish water body with consequent silting and
554 evaporation if freshwater inputs do not overprint the RSL signal. This led to considerable
555 shallowing and silting of the semi-enclosed lagoons compared to the open lagoons. The
556 depth of these lagoons seldom exceeds a few decimetres (Ruiz et al., 2006). In the
557 micropalaeontological assemblage of the SAM9 core, this corresponds to the first clear
558 inputs of freshwater fauna (*I. bradyi* and *E. virens*) and the first disappearance of foraminifera
559 (Figs. 4, 8).

560 Arboreal pollen of mesophilous taxa possibly refers to a relict plain forest, growing in the
561 coastal humid area and dominated by oaks tolerant of wet soils (*Quercus robur* L.). A
562 deciduous oak forest associated with thermophilous elements, such as *Quercus*
563 *ilex* (evergreen oak), *Ostrya carpinifolia* and/or *Carpinus orientalis* (hornbeams), and *Fraxinus*
564 *ornus* (manna ash), also covered the study area up to the slopes of the southern Apennines,
565 bordering the "Capitanata" to the west. The co-occurrence of deciduous trees with thermo-
566 xerophilous species from different bioclimatic zones is typical of the Apulian woodlands
567 (Russo and Strizzi, 2013). Moreover, evergreen oaks could have been part of the xerophilous
568 vegetation, such as the Mediterranean *maquis* formations of *Quercus*, *Olea*
569 (olive), *Pistacia* (pistachio), and Ericaceae (heather). These vegetation types characterised
570 the Apulia region (Lago Battaglia - Caroli and Caldara, 2007; Lago Salso - Di Rita et al., 2011;
571 Lago Alimini Piccolo - Di Rita and Magri, 2009), as well as other contemporary coastal areas
572 in Sicily (Noti et al., 2009; Tinner et al., 2009) and along the Tyrrhenian coast (Di Donato et

573 al., 2008; Sadori et al., 2010; Bellotti et al., 2016; Russo Ermolli et al., 2018; Sadori et al., 2016;
574 Di Rita et al., 2018a; 2018b; Vignola et al., 2022). Among mountain taxa recognised in the
575 SAM9 core (Fig. 5), *Fagus* (beech) sparse pollen grains are likely from the Gargano
576 Promontory, where this broadleaved tree forms a dense forest below its common altitudinal
577 belt (Hoffmann, 1961).

578 Of note is also the sparse presence of *Abies* (fir) pollen from ca. 5 ka cal BP to 3.1 ka cal BP.
579 The silver fir (*A. alba* Mill.) is tolerant to dry conditions and is still recorded in the mountains
580 of the Calabria region (South Italy) and even along the Tyrrhenian coasts of Northern and
581 Central Italy during the early-mid Holocene (Colombaroli et al., 2007, 2008; Bellini et al.,
582 2009). As the potential spatial range of *A. alba* also include the northern part of Apulia
583 (Tinner et al., 2013), the occurrence of this conifer in the Salpi lagoon cannot be excluded. In
584 this context, the role of the Gargano Promontory as a post-glacial refugium for altitudinal
585 trees (beech and fir) can be hypothesised. Another possibility is the transport of *Abies* pollen
586 from the southern Apennines, where it was abundant until ca. 3 ka BP (Allen et al., 2002;
587 Joannin et al., 2012). The other mountain trees occur only sporadically and probably
588 originated from a greater distance, both from the Italian Apennines (e.g. *Betula*; see the
589 pollen record of Lago Grande di Monticchio, Allen et al., 2002) and exceptionally from the
590 Balkans (e.g. *Picea* which is not present in Southern Italy; see the pollen record of Lake
591 Shkodra, Albania, Sadori et al., 2015). This evidence and interpretation is confirmed by their
592 occurrence even in the palynological sequence of Lago Alimini Piccolo (Di Rita and Magri,
593 2009).

594 *Pinus* pollen is not abundant in the SAM9 core record, suggesting that pinewoods were not
595 widespread in the Tavoliere plain, but were restricted to the northern side of the Gargano
596 Promontory (Lago Battaglia - Caroli and Caldara, 2007).

597 Towards the end of the Northgrippian (4.2 ka BP), AP percentage and concentration values
598 abruptly decrease, whilst NAP percentage increases (Figs. 5, 6). This indicates a decline in
599 forest cover. As anthropogenic pollen indicators are scant (Fig. 5), such deforestation is
600 interpreted as a regional event, most probably caused by the arid conditions that the
601 Mediterranean basin experienced at around 4.2 ka BP (Bini et al., 2019; Di Rita and Magri,
602 2019; Di Rita et al., 2022). A similar decline in broadleaved vegetation, accompanied by an
603 opening of the landscape, is attested throughout Apulia before 4 ka BP (Caroli and Caldara,

604 2007; Di Rita and Magri, 2009). It is possible that this climatic episode contributed to the
605 further lowering of the water table in the southern sector of the Salpi lagoon, paving the
606 way to the colonisation of halophytic herbs during the Early Meghalayan.

607 5.2. Early Meghalayan (4.2 ka–2.4 ka BP)

608 During the early phases of the Meghalayan (Fig. 9b), facies analysis in the SAM9 core shows
609 the closure of the lagoon and the formation of a marsh environment (Fig. 7), indicating a
610 reduction in the water table, the steady-progressive retreat of the lagoon, as well as a
611 decrease in salinity. These conditions reflect the aforementioned continuous development
612 of the beach barrier, prograding up to the northern sector of the Salpi lagoon during the 4.2
613 ka BP dry climatic event (Di Rita et al., 2011). The dunes most likely isolated the back-coastal
614 areas and promoted the formation of marshy wetlands, especially in the inner sector of the
615 coastal plain. Conversely, floodplain progradation can be observed in the innermost part of
616 the coastal plain, as shown by cores SAL2 and SAM1 (Fig. 7). Conversely, the fauna of the
617 cores from Coppa Nevigata (Caldara et al. 2003, Caldara and Simone, 2005) display a strong
618 marine influence, both in the foraminifera (*A. beccari*, *H. germanica*, *Porosonion granosum*,
619 *Elphidium oceanensis*, *Rosalina bradyi* and *R. floridensis*), as well as among the ostracoda (*C.*
620 *torosa*, *Loxoconcha elliptica*, *Leptocythere* spp., *Propontocypris pirifera*) and the molluscs
621 (*Cerastoderma glaucum*, *Abra segmentum*, *Ciclope nerite*, *Loripes lacteus*). Caldara and Simone
622 (2005) identified a lagoonal environment (*Hydrobiidae* spp. and *Cerastoderma* lagoon) that
623 spans from 3.6 ka BP to 2.8 ka BP, thus indicating open marine lagoon conditions in the
624 northern area of the coastal plain.

625 The freshwater input is clearly recorded by the ostracod assemblage of SAM9 core (Fig. 8).
626 Indeed, the relevant OEG is freshwater. ~~The dominant species, *I. bradyi* and *H. salina*,~~
627 ~~indicate low-energy waters and a maximum salinity of 4-5‰.~~ The periodic increase in
628 ostracod **freshwater** species during this time span is alternated with peaks of
629 Amaranthaceae (in both pollen percentage and pollen concentration; Figs. 5, 6), indicating
630 that halophytic vegetation continued to dominate such patchy shallow-water environments
631 (Fig. 8). As at the same time the AP concentration values tend to be nought (Fig. 6), it can be
632 argued that the SAM9 core records indicate an open landscape with an over-representation
633 of local halophytes, probably due to increasing aridity and the definitive replacement of the
634 former plain forest with a saltmarsh.

635 The rapid expansion of saltmarsh herbs, combined with water level changes and fostered
636 by the climatic exacerbation at the early stages of the Meghalayan, is a regional event
637 recorded in the Salpi lagoon and surrounding areas (Caroli and Caldara, 2007; Di Rita et al.,
638 2011; Di Rita, 2013). These data confirm the onset of drier climatic conditions along the
639 Apulian coast during the 4th millennium BP, although palaeoclimatic records from the
640 Adriatic Sea points out rapid fluctuations (Piva et al., 2008; Siani et al., 2013).

641 Arboreal pollen from the SAM9 core reveals that the woodland in the study area did not
642 recover after the opening at 4.2 ka BP, unlike at Coppa Nevigata (Caldara et al., 2003) and
643 in other part of Southern Italy (Noti et al., 2009; Tinner et al., 2009; Calò et al., 2012; Di Rita
644 et al., 2018b), where an increase of evergreen taxa is recorded. In the southern part of the
645 Salpi lagoon, the mixed deciduous and evergreen oak forest was replaced by an almost
646 treeless open landscape with scattered Mediterranean shrubs and trees (*Pistacia*, *Quercus ilex*
647 type; Fig. 5), which persisted up to the present (see also concentration values in Fig. 6). This
648 was most probably due to continuous human activities from the Bronze Age onwards,
649 affecting a transitional environment under semi-arid conditions. Indeed, during this period,
650 archaeological records show a strong intensification of settling, when many sites are
651 documented along the Northern Adriatic coast and at key inland locations (Cazzella et al.,
652 2017). The high frequency of fires, evidenced by the peaks of charcoal concentration (Fig. 6),
653 could have been favoured by the climatic change, although an anthropogenic source cannot
654 be ruled out. In fact, concomitantly to the largest class of charcoal fragments, the presence
655 of pollen of ruderal plants (nitrophilous *Urtica*, up to 8%; Fig. 5) testifies to an anthropogenic
656 environment, thus confirming the human frequentation of the lagoon during the Bronze
657 Age. However, in the absence of the primary anthropogenic pollen indicators (i.e. cereals,
658 *Olea*), it is possible that the marshland was not cultivated. An exception is the pollen of
659 *Juglans* (walnut), whose occurrence in pollen sequences of Southern Italy starting around
660 2.7 ka BP has been interpreted as an indication of the widespread use of walnut in Greek
661 and Roman times (Sadori, 2013). The earlier attestation in the SAM9 core (ca. 3 ka BP, Fig.
662 5) is noteworthy, although the presence of walnut in pollen samples from other Apulian
663 areas dated to 6 ka BP onwards (Di Rita and Magri, 2009; Di Rita et al., 2011) argue for
664 Mediterranean populations growing in glacial refugia (Pollegioni et al., 2017).

665 Between 3.2 ka and 2.4 ka BP, the age-depth model of the SAM9 core testifies to a higher
666 sedimentation rate (Fig. 8). This increase could be attributed to a) cold climate phases
667 occurring at 3.5 ka–3.2 ka BP and 2.6 ka–2.3 ka BP (Orombelli and Pelfini, 1985; Haas et al.,
668 1998), also recognised in the Adriatic Sea and the Aegean Sea as the most recent Adriatic
669 cooling event (Sangiorgi et al., 2003) or b) anthropic deforestation and short-term
670 hydrological changes due to enhanced runoff processes. Regardless of the natural- or
671 human-induced cause, the sedimentary accretion in alluvial plains appears to overwhelm
672 the rate of relative sea-level rise, forcing lagoonal and brackish environments to a freshening
673 of water due to a surplus of sediment supply (Nichols, 1989).

674 Caldara and Simone (2005) found many preserved organic materials in the sediment core
675 closest to the archaeological site of Coppa Nevigata, dated to before 3 ka BP and interpreted
676 as product of a rapid sediment accumulation caused by wash over. On the other hand,
677 Caldara et al (2003) identified a sedimentation gap between 3.110 ± 50 and 370 ± 50 BP, related
678 to arid phases and aquifer depletion. Pollen data of Lago Battaglia also testifies to the
679 increased sediment deposition and the spread of Cyperaceae at the expense of halophytic
680 vegetation during this period (Caroli and Caldara, 2007).

681 At around 2.8 ka BP, a spike of *C. torosa* marks a clear increase in salinity, which is confirmed
682 by the occurrence of *A. tepida* and *H. germanica* (Fig. 8). Conversely, grain size analysis
683 highlights a stable silty/clay ratio, pointing to overbank deposits possibly remobilised in
684 the lagoonal environment due increased sediment inflow from the Carapelle River (Fig. 4).
685 At the same time, pollen grains from hygrophilous herbs and riparian-emergent
686 macrophytes (i.e. Cyperaceae and *Typha angustifolia* type) periodically increase. In addition,
687 the cyanobacterium *Gloeotrichia* colonised the marsh environments to a fluctuating extent,
688 as clearly indicated by the concentration peak at ca. 2.7 ka BP (Fig. 8). This filamentous
689 cyanobacterium contributes to nutrient-poor eutrophication of lakes by transferring
690 phosphates into the water (Stevenson, 1996; Kornijów et al., 2016). Thus, the increase in
691 salinity is linked to evaporation processes and water shallowing under dry climate
692 conditions, which have also contributed to the waves of expansion of Amaranthaceae.

693 The virtual disappearance of *Fagus* from the record after ca. 2.8 ka BP (only one pollen grain
694 came from the sample dated to ca. 2190 BP) indicate the reduction of the Gargano beech
695 forest due to the onset of drier conditions through the Meghalayan. This evidence is

696 confirmed by pollen data from the northern side of the Gargano Promontory (Caroli and
697 Caldara, 2007). The same trend is seen in the *Abies* curve, whose last attestation is dated to
698 ca. 3090 BP (Fig. 5). Since the decline of *Abies* in Lago Grande di Monticchio occurs
699 simultaneously (Allen et al., 2002), it is probably a combination of climate change and
700 human exploitation.

701 Archaeologically, during the Iron Age, the Tavoliere coastal plain experienced the
702 emergence of new centres (Figg. 8, 9b). The settlement of *Cupola-Beccarini* (Daunian
703 *Sipontum*) is attested from the 7th cent. BCE, whilst *Salpia Vetus* developed in the 10th cent.
704 BCE. The latter was hypothesised to be surrounded by brackish waters (Lippolis and
705 Giammatteo, 2008) and benefited from a favourable position, surrounded and protected by
706 water to the north, whilst defended to the south by a bank with a ditch, built between the
707 7th and the 6th cent. BCE. Moreover, in his description of coastal Daunia (Northern Apulia),
708 the Greek geographer Strabo pointed out that *Salpia* was located near a navigable river,
709 most probably the Carapelle River, and a "*stomalimne megale*" (roughly translated as "big
710 estuary") through which the grain was traded seaward from other areas of the coastal plain.
711 Thus, this description may be a reference to a connection between the Carapelle River and
712 the coastal lagoon.

713 5.3. Late Meghalayan (2.4 ka-0.2 ka BP)

714 During the last part of the Holocene, facies analysis of the SAM9 core shows that wetlands
715 had already developed into floodplain environments (Fig. 7). However, in the SAM8 core,
716 drilled a few metres away from the SAM9 core, the persistence of marshlands indicate that
717 the area continued to be affected by seasonal flooding. The latter were most probably
718 influenced by the migration of the Carapelle River within the coastal plain. In fact, Caldara
719 et al. (2002) reported that the lagoon experienced a sudden increase in turbidity of the main
720 inflowing rivers, particularly from the Carapelle River, which resulted in the separation of
721 the Salpi lagoon into two minor basins (Fig. 9c), lately named Lago Salso (north) and Lago
722 Salpi (south). The development of a floodplain is well recorded by the ostracod assemblage,
723 where the euryhaline taxa disappear, and *L. inopinata* and *E. virens* occur (Fig. 8). These
724 species are common in shallow waters, including temporary ponds, swamps, lakes, and
725 rivers, with a salinity tolerance of 9‰ and 5‰ respectively (Meisch, 2000). The occurrence
726 of ehippia *Daphnia*-type and abundant pharyngeal teeth of Cyprinids are recorded in the

727 SAM9 core as well as in the upper part of the SAL2 core, where *C. ophthalmica*, *I. bradyi*, *H.*
728 *brevicaudata* and *P. zenkeri* also occur. This assemblage describes shallow, low-energy waters
729 rich in aquatic vegetation, as attested also in the pollen data by the increase of *Typha*
730 *angustifolia* type, *Typha latifolia* type and ferns (Fig. 5).

731 Pollen data from SAM9 core confirms a patchy scenario (Fig. 8). Amaranthaceae declined
732 abruptly as riverine inputs and shallower waters were accompanied by a decrease in
733 salinity, fostering the growth of macrophytes, ferns, and green algae living in shallow
734 waters (Fig. 8). At the same time, new areas were colonised by herbs from the open
735 landscape tolerant to xeric conditions. In addition, NPPs such as *Glomus*, a mycorrhizal
736 fungus, and *Pseudoschizaea* testify to the increase in erosional processes on the drylands due
737 to the combination of semi-arid climate conditions, deforestation, and human pressure
738 already postulated since the beginning of the Meghalayan (Fig. 8). These factors acted on a
739 regional scale, as a similar change in the palaeoenvironment (i.e. the expansion of aquatic
740 and dryland taxa) can also be traced in the record of Lago Battaglia during the same
741 period (Caroli and Caldara, 2007). In this regard, anthropogenic pollen indicators in the
742 SAM9 core show that local communities benefited from this landscape change. Since ca.
743 2350 BP (4th cent. BCE), the inland was exploited for pastoral activities, as indicated mainly
744 by pollen of Cichorieae (the chicory family) among xeric vegetation, which includes
745 nitrophilous herbs resistant to animal trampling (Florenzano, 2019). Asteroideae, Poaceae,
746 and *Plantago*, whose pollen grains are strongly present in the upper part of the core, are also
747 indicators of pasturelands (Behre, 1981), bolstering support for 5th-4th cent. BCE (2450-2350
748 BP) breeding in Daunia revealed by the archaeological record (Buglione et al. 2016).

749 The slight increase in *Olea* pollen at ca. 2.4 ka BP (4th cent. BCE) could be linked to the
750 expansion of olive groves inland. Although olive is a natural component of the
751 Mediterranean *maquis*, the overall scarcity of this taxon in the previous levels suggests that
752 its occurrence coincides with human exploitation of the area. The only occurrence of
753 *Castanea* (chestnut) pollen (1%) at ca. 2190 BP (half 3rd cent. BCE) is noteworthy, since this
754 plant, together with walnut, was frequently spread by humans across the Italian peninsula
755 since ca. 2700 BP (Mercuri et al., 2013). Apiaceae (the carrot family) and Brassicaceae (the
756 cabbage family), whose pollen reaches significant values during this period, could also
757 represent cultivated herbs. In fact, they include plants poorly represented in natural pollen

758 deposits due to their entomophilous pollination, but have a crucial economic value as
759 vegetable-garden and aromatic species. In particular, cabbages have been known as one of
760 the most common vegetables in Southern Italy since pre-Roman times (Russo Ermolli et al.,
761 2014; Vignola et al., 2022). Cereal pollen is absent during this period, although pollen grains
762 of weedy plants such as *Centaurea* are attested since ca. 2900 BP (half 10th cent. BCE, Fig. 5).
763 The evidence of human exploitation as highlighted by SAM9 core pollen recorded before
764 the Roman occupation is consistent with other palaeoenvironmental and historical data for
765 the region.

766 Evidence of local cereal cultivation (e.g. *Hordeum* group: 8%; Fig. 5) in the SAM9 core starts
767 around 1850 BP during the Roman period. Since cereals are very low-pollen producers, it is
768 possible that fields reached the former wetland. *Olea* disappears, while Cichorieae and
769 Brassicaceae increase strongly (Fig. 5). These data indicate a highly anthropogenic landscape
770 of pastures, cultivated fields, and vegetable gardens, typical of Roman agriculture (Vignola
771 et al., 2022). From ca. 1460 BP (end of 5th cent. CE, Late Antiquity), cereal pollen
772 (*Avena/Triticum*, *Hordeum* group, *Secale*; Fig. 5) occurs along with walnut and olive,
773 although the latter does not reach a significant amount (3%, Fig. 5). Because of a low
774 percentage in the upper part of the SAM9 core, the presence of *Olea* and other natural
775 components of Mediterranean *maquis* (i.e. *Pistacia*, *Ephedra*, Ericaceae, Fig. 5) could be
776 related to the progressive expansion of shrublands due to continuous woodland clearance.
777 The fact that such vegetation development could be both natural- and human-induced is
778 confirmed by the exponential increase in percentage and concentration values of Cichorieae
779 up to the Middle Ages (Figs. 5, 6). The peak of charcoal concentration at ca. 1460 BP seems
780 to confirm the intensification of anthropic fires, as demonstrated in the southwestern
781 portion of the Tavoliere Plain (Heim, 1995; Marchesini et al., 1995; Caracuta and Fiorentino,
782 2009). On the other hand, the area of Lago Alimini Piccolo experienced a more intensive
783 exploitation of olive trees from the 6th century CE (1450-1350 BP) up to the present-day (Di
784 Rita and Magri, 2009).

785 The conditions of the coastal plain appear to be stable throughout the Roman period
786 onwards. Nevertheless, a deep transformation of the settlement strategies took place
787 between the 1st and 2nd cent. CE (2050-2150 BP). Vitruvius reports that the area
788 surrounding *Salpia Vetus* became insalubrious and unhealthy. For this reason, the

789 population selected a new location for this city -Roman *Salapia* -adjacent to the southern half
790 of the lagoon system, in a more elevated area, and thus potentially protected from malaria
791 breeding. Historical data, however, does not correspond with that of the pollen. Evidence
792 of cereal cultivation is attested in the SAM9 core proximate to the pre-Roman city until ca.
793 780 BP (1170 CE, Fig. 5) signalling continued agricultural exploitation in this zone rather
794 than a complete takeover by unhealthy, marsh-like conditions. The reconstruction is even
795 more complex when considering sedimentological data from the other drillings. In fact, the
796 SAM5 and SAM6 cores indicate that eastward of the re-founded city of Medieval *Salpi*, the
797 area was dominated by marshes from the 3rd cent. CE (1640-1539 cal BP) until the 16th cent.
798 CE (476-312 cal BP), a trend which perhaps can be traced back to the founding of the Roman
799 town in the 1st cent. BCE. These are hardly the “ideal” conditions expected for a new town
800 supposedly fleeing an unhealthy marsh, if the perspective on marshes is wholly negative.
801 Rather, a more nuanced understanding of the benefits of life adjacent to a marsh must be
802 considered for the inhabitants of Roman *Salapia*, as do the ways the settlements was
803 positioned in and negotiated with the surrounding environment. In fact, the western part
804 of the city was characterised by floodplains, as shown by SAL3 and SAM4 cores, a
805 distinction in elevation that would have produced the kind of drainage possibilities that
806 Vitruvius advocates for in marshy areas, perhaps indication of more healthful conditions
807 than those found contemporaneously at *Salpia Vetus*.

808 6. Conclusions

809 The ~~high-resolution~~ palaeoenvironmental analyses, coupled with archaeological and
810 historical data, provides for the first time new insights regarding the evolution of the
811 southern margin of the Salpi lagoon. In particular, it has enabled outlining and refining the
812 understanding of its evolution from the Late Northgrippian up to the last part of the
813 Meghalayan. Until now, the bulk of knowledge of the processes involved in the evolution
814 of the Tavoliere coastal plain was focused on the northern part of the coastal plain, whilst
815 the southern margin remained poorly investigated.

816 As a result of this research, several conclusions can be drawn, as follows:

- 817 – ~~Drilling~~ data from the southern margin of the Tavoliere coastal plain show a general
818 regressive trend of the Salpi lagoon, indicated by a vertical stacking of swamp and

- 819 alluvial deposits over lagoonal facies. This highlights the progressive reduction of the
820 lagoon, and the seaward progradation of swampy and floodplain environments up to
821 the definitive emersion of most of the landscape.
- 822 – Stratigraphic analysis of the cores, coupled with ostracod analyses and radiocarbon
823 calibrated ages, allowed a detailed reconstruction of the facies association and the
824 identification of the three main palaeoenvironmental changes from the onset of the
825 regression of the lagoon to the last phase of the Meghalayan. The lagoon was partially
826 connected to the sea between 5.5 ka and 4.2 ka BP (Late Northgrippian). Between 4.2 ka
827 and 2.4 ka BP (Early Meghalayan), the development of marshes and swamps with
828 restricted brackish lagoon conditions and permanent freshwater input is recorded,
829 possibly a consequence of increased river influx and continuous development of the
830 dune barrier. Between 2.4 ka BP to present, the continuous freshwater influx from the
831 Carapelle River caused the rapid progradation of the floodplain into the coastal plain
832 and the closure of the lagoon, with the formation of the two coastal lakes of Lago Salso
833 (north) and Lago Salpi (south).
- 834 – Pollen data confirm the palaeoenvironmental evolution of the lagoon, with the
835 expansion of halophytic herbs under local brackish conditions during the Early
836 Meghalayan and the exponential spread of herbs from drylands in correspondence with
837 the closure of the basin. The emersion of the land during the last phase enabled the
838 intensive exploitation of the area and the establishment of a highly anthropogenic
839 landscape, consisting mainly of pastures and cultivated fields from the Roman period
840 onwards. At a regional scale, the forest cover gradually decreased due to an aridification
841 trend, documented in Apulia since 4.2 ka BP, whilst the enhanced human activities
842 contributed to a deforestation process from the Hellenistic period to the Middle Ages.
- 843 – The comparison between the cores on the southern margin of the Salpi lagoon and the
844 archaeological areas of Coppa Nevigata indicates an asynchronous evolution of the
845 lagoonal facies, linked to the different development of the sand barriers and the
846 different inputs of the main rivers crossing the "Capitanata" plain, in particular the
847 Carapelle River and Candelaro River.
- 848 – Although the sedimentological, chronological and micropalaeontological data do not

849 provide detailed reconstruction of the major phases of floodplain progradation or
850 retreat that may have occurred from Roman to Medieval times, it is assumed that coastal
851 lakes and marshlands have survived before the extensive land reclamation project that
852 took place at the beginning of the 20th cent. CE. Such environmental conditions were the
853 main cause which triggered the decision of the inhabitants of *Salpia Vetus* to establish
854 the settlement of *Salapia*. This newly occupied sector of the coastal plain was far from
855 the influence of the Carapelle River and closer to the sea, therefore potentially protected
856 from malaria breeding.

857 **Author contributions**

858 **Davide Susini:** Facies analysis, Images, Tables, Writing-Original draft preparation;
859 **Cristiano Vignola:** Pollen analysis, Images, Writing-Reviewing; **Roberto Goffredo:** Project
860 co-director; Archaeological background, Writing-Reviewing; **Darian Marie Totten:** Project
861 co-director, Archaeological background, Writing-Reviewing; **Alessia Masi:** Pollen analysis,
862 Images, Writing-Reviewing; **Alessandra Smedile:** Foraminifera analysis, Images, Writing-
863 Reviewing; **Paolo Marco De Martini:** Coring, Facies analysis; **Francesca Romana Cinti:**
864 Facies analysis, Writing-Reviewing; **Laura Sadori:** Writing-Reviewing; **Luca Forti:** Coring,
865 Grain size analysis; **Girolamo Fiorentino:** Archaeological background, Writing-Reviewing;
866 **Andrea Sposato:** Coring, Grain size analysis, Facies analysis; **Ilaria Mazzini:** Ostracods
867 analysis, Images, Writing-Reviewing.

868 All authors were involved in the discussion and approved the final version of the
869 manuscript.

870 **Data availability**

871 Remote images, and digital models used for the basemaps in Figures 1, 2, and 9 are free-
872 downloaded from the SIT portal of the Apulia region
873 (http://www.sit.puglia.it/portal/sit_portal). The geomorphological features in Figures 1
874 and 9 were digitally mapped in ArcGIS© environment and modified from the Geological
875 Survey of Italy for the Geological Map of Italy at the scale 1:50.000, CARG Project
876 (<https://www.isprambiente.gov.it/Media/carg/index.html>), and the Geological map of
877 Italy at the scale 1:100.000

878 (<https://www.isprambiente.gov.it/en/services/cartography/geological-and-geothematic-maps/geological-map-at-a-scale-1-to-100000>).

880 **Declaration of competing interest**

881 The authors declare that they have no known competing financial interests or personal
882 relationships that could have appeared to influence the work reported in this paper.

883 **Acknowledgements**

884 This research has been funded by The National Endowment for the Humanities: Democracy
885 demands wisdom (USA), Collaborative Grant program (grant number RZ-249965-16),
886 awarded for the term 2017–2020, to the Life on the Lagoon: Reconstructing the Biography
887 of Human-Landscape Dynamics on the Salpi Lagoon, Italy project, co-directed by R.
888 Goffredo and D.M. Totten. Any views, findings, conclusions, or recommendations
889 expressed in this article do not necessarily represent those of the National Endowment for
890 the Humanities. The 2017 coring campaign has been performed by the SONDAG srl under
891 the supervision of dr. Giorgio de Giorgio. We thank Francesco Versino for his precious work
892 on processing the samples from the cores.

893 **References**

- 894 Allen, J.R.M, Watts, W.A, McGee, E, Huntley, B., 2002. Holocene environmental
895 variability – the record from Lago Grande di Monticchio, Italy. *Quaternary*
896 *International* 88, 69–80. [https://doi.org/10.1016/S1040-6182\(01\)00074-X](https://doi.org/10.1016/S1040-6182(01)00074-X)
- 897 Amorosi, A., Bini, M., Giacomelli, S., Pappalardo, M., Ribecai, C., Rossi, V., Sammartino, I.,
898 Sarti, G., 2013. Middle to late Holocene environmental evolution of the Pisa coastal
899 plain (Tuscany, Italy) and early human settlements. *Quaternary International* 303, 93–
900 106. <https://doi.org/10.1016/j.quaint.2013.03.030>
- 901 Andersen, S.T., 1979. Identification of wild grass and cereal pollen [fossil pollen, Annulus
902 diameter, surface sculpturing]. *Danmarks Geologiske Undersoegelse (Denmark)*,
903 *Aarbog*.
- 904 Andronico, D., Cioni, R., 2002. Contrasting styles of Mount Visuvius activity in the period
905 between the Avellino and Pompeii Plinian eruptions, and some implications for

- 906 assessment of future hazards. *Bulletin of Volcanology* 64, 372–391.
907 <https://doi.org/10.1007/s00445-002-0215-4>
- 908 Barker, G., Biagi, P., Castelletti, L., Cremaschi, M., Nisbet, R., 1987. Sussistenza, economia
909 ed ambiente nel neolitico dell'Italia settentrionale. *Atti della XXVI Riunione Scientifica*
910 dell'IIPP, Firenze, pp. 103–118.
- 911 Battista, C., Caldara, M., Pennetta, L., Zito, G.M., 1993. Analisi dell'aridità del clima nel
912 Tavoliere di Puglia. *Bonifica* 8, 67–72.
- 913 Battista, C., Caldara, M., Pennetta, L., Zito, G.M., 1994. Evoluzione del lago di Salpi fra
914 clima e interventi antropici. In: Piccione, V., Antonelli, C., Guerrini, C. (eds.), *Atti III*
915 *Workshop Del Progetto Strategico: Clima Ambiente e Territorio*, Potenza, 1990, Vol.2.
916 Italian National Research Council, Rome, pp. 155–178.
- 917 Behre, K.E., 1981. The interpretation of anthropogenic indicators in pollen diagrams.
918 *Pollen Spores* 23, 225–245.
- 919 Bellini, C., Mariotti-Lippi, M., Montanari, C., 2009. The Holocene landscape history of the
920 NW Italian coasts. *The Holocene* 19, 1161–1172.
921 <https://doi.org/10.1177/0959683609345077>
- 922 Berglund, B.E., Ralska-Jasiewiczowa, M., 1986. Pollen analysis and pollen diagrams. In:
923 Berglund, B.E. (ed.), *Handbook of Holocene Palaeoecology and Palaeohydrology*. John
924 Wiley & Sons, Chichester, pp. 455–496.
- 925 Beug, H.-J., 2004. *Leitfaden der Pollenbestimmung*. Pfeil, München.
- 926 Bini, M., Zanchetta, G., Perşoiu, A., Cartier, R., Català, A., Cacho, I., et al., 2019. The
927 4.2 ka BP Event in the Mediterranean region: an overview. *Climate of the Past* 15, 555–
928 577. <https://doi.org/10.5194/cp-15-555-2019>
- 929 Biscotti, N., 2001. I valori botanici del Gargano. *Informatore Botanico Italiano* 33, 289–291.
- 930 Boenzi, F., Caldara, M., Moresi, M., Pennetta, L., 2001. History of the Salpi lagoon-sabha
931 (Manfredonia Gulf, Italy). *Il Quaternario* 14, 93–104.
- 932 Boenzi, F., Caldara, M., Pennetta, L., 1991. Osservazioni stratigrafiche e geomorfologiche
933 nel tratto meridionale della piana costiera del Tavoliere di Puglia. *Geografia Fisica e*
934 *Dinamica Quaternaria* 14, 23–31.

- 935 Boenzi, F., Caldara, M., Pennetta, L., Simone, O., 2006. Environmental Aspects Related to
936 the Physical Evolution of Some Wetlands Along the Adriatic Coast of Apulia
937 (Southern Italy): a Review. *Journal of Coastal Research* 1, 170–175.
- 938 Bronk Ramsey, C., 2009. Bayesian Analysis of Radiocarbon Dates. *Radiocarbon* 51, 337–
939 360. <https://doi.org/10.1017/S0033822200033865>
- 940 Buffardi, C., Barbato, R., Vigliotti, M., Mandolini, A., Ruberti, D., 2021. The Holocene
941 Evolution of the Volturno Coastal Plain (Northern Campania, Southern Italy):
942 Implications for the Understanding of Subsidence Patterns. *Water* 13, 2692.
943 <https://doi.org/10.3390/w13192692>
- 944 Buglione, A., De Venuto, G., Volpe, G., 2016. Agricoltura e allevamento nella Puglia
945 settentrionale tra età romana e Medioevo: il contributo delle bioarcheologie. *Mélanges*
946 *de l'École française de Rome - Antiquité* 128. <https://doi.org/10.4000/mefra.3475>
- 947 Calanchi, N., Dinelli, E., 2008. Tephrostratigraphy of the last 170 ka in sedimentary
948 successions from the Adriatic Sea. *Journal of Volcanology and Geothermal Research*
949 177, 81–95. <https://doi.org/10.1016/j.jvolgeores.2008.06.008>
- 950 Caldara, M., 1996. Aspetti di geologia ambientale e di morfologia costiera in alcuni tratti
951 del litorale nord-barese. *Geologi* 96, 39–61.
- 952 Caldara, M., Caroli, I., Simone, O., 2004. Geomorphological changes due to human actions
953 at Coppa Navigata (Tavoliere di Puglia, Southern Italy) reconstructed through core
954 analyses. *Il Quaternario* 17, 495–508.
- 955 Caldara, M., Cazzella, A., Fiorentino, G., Lopez, R., Magri, D., Moscoloni, M., Narcisi, B.,
956 Simone, O., 2003. The relationship between Coppa Navigata settlement and the
957 wetland area during the Bronze Age (south-eastern Italy). In: Fuoache, E. (ed.), *The*
958 *Mediterranean World Environment and History*. Elsevier, Paris, pp. 429–438.
- 959 Caldara, M., Pennetta, L., 1990. Evoluzione dell'ambiente olocenico nel basso Tavoliere di
960 Puglia. *Bonifica* 6, 47–66.
- 961 Caldara, M., Pennetta, L., 1992. Interpretazione paleoclimatica di dati preistorici e storici
962 relativi all'entroterra del Golfo di Manfredonia. *Memorie della Società Geologica*
963 *Italiana* 42, 197–207.

- 964 Caldara, M., Pennetta, L., 1993a. Ambienti aridi del tipo 'Sabkha' nei sedimenti olocenici
965 della piana costiera fra Manfredonia e Zapponeta. *Bonifica* 8, 73–82.
- 966 Caldara, M., Pennetta, L., 1993b. Nuovi dati per la conoscenza geologica e morfologica del
967 Tavoliere di Puglia. *Bonifica* 8, 25–42.
- 968 Caldara, M., Pennetta, L., Simone, O., 2002. Holocene Evolution of the Salpi Lagoon
969 (Puglia, Italy). *Journal of Coastal Research* 36, 124–133. [https://doi.org/10.2112/1551-
970 5036-36.sp1.124](https://doi.org/10.2112/1551-5036-36.sp1.124)
- 971 Caldara, M., Simone, O., Porzia, S., 2003. L'aera umida di Coppa Nevigata tra Neolitico e
972 l'Età del Bronzo. Atti del 23° Convegno Nazionale sulla Preistoria, Protostoria e Storia
973 della Daunia, S. Severo 23–24 Novembre 2002. Stabilimento Litografico Centografico
974 Francescano, Foggia, 203–230.
- 975 Caldara, M., Simone, O., 2005. Coastal changes in the eastern Tavoliere Plain (Apulia,
976 Italy) during the Late Holocene: Natural or anthropic? *Quaternary Science Reviews* 24,
977 2137–2145. <https://doi.org/10.1016/j.quascirev.2004.08.024>
- 978 Caldara, M., Simone, O., 2012. L'ambiente fisico nell'area dell'insediamento di Coppa
979 Nevigata. In: Cazzella, A., Moscoloni, M., Recchia, G. (eds.), *Coppa Nevigata e l'area
980 umida alla foce del Candelaro durante l'età del Bronzo*. Claudio Grenzi Editore, pp.
981 339–359.
- 982 Calò, C., Henne, P.D., Curry, B., Magny, M., Vescovi, E., La Mantia, T., Pasta, S., Vannièr,
983 B., Tinner, W., 2012. Spatio-temporal patterns of Holocene environmental change in
984 southern Sicily. *Palaeogeography, Palaeoclimatology, Palaeoecology* 323–325, 110–122.
985 <https://doi.org/10.1016/j.palaeo.2012.01.038>
- 986 Caracuta, V., Fiorentino, G., 2009. L'analisi archeobotanica nell'insediamento di Faragola
987 (FG): il paesaggio vegetale tra spinte antropiche e caratteristiche ambientali, tra
988 tardoantico e altomedioevo. In: Volpe, G., Favia, P. (eds), *V Congresso Nazionale di
989 Archeologia Medievale (Foggia-Manfredonia, 30 settembre-3 ottobre 2009)*. Firenze,
990 717–726.
- 991 Carmona, P., Ruiz-Pérez, J.-M., Blázquez Morilla, A.M., López-Belzunce, M., Riera, S.,
992 Orengo, H., 2016. Environmental evolution and mid-late Holocene climate events in

- 993 the Valencia lagoon (Mediterranean coast of Spain). *The Holocene* 26, 1750–1765.
994 <https://doi.org/10.1177/0959683616645940>
- 995 Caroli, I., Caldara, M., 2007. Vegetation history of Lago Battaglia (eastern Gargano coast,
996 Apulia, Italy) during the middle-late Holocene. *Vegetation History and*
997 *Archaeobotany* 16, 317–327. <https://doi.org/10.1007/s00334-006-0045-y>
- 998 Cazzella, A., Moscoloni, M., Recchia, G., 2012. Coppa Nevigata e l'area umida alla foce del
999 Candelaro durante l'Età del Bronzo. Grenzi Editore, Foggia.
- 1000 Cazzella, A., Recchia, G., Tunzi, A.M., 2017. La Puglia tra Bronzo Antico e Bronzo Recente.
1001 In: Radina, F. (ed.), *Preistoria e Protostoria della Puglia, Studi di Preistoria e*
1002 *Protostoria - 4*. Istituto italiano di preistoria e protostoria, Firenze, pp. 431–442.
- 1003 Ciccone, S., 1984. Cinquant'anni di bonifica nel Tavoliere. Bastogi, Foggia, Italy.
- 1004 Cocchi, L., Stefanelli, P., Carmisciano, C., Caratori Tontini, F., Taramaschi, L. and Cipriani,
1005 S., 2012). Marine Archaeogeophysical Prospection of Roman Salapia Settlement
1006 (Puglia, Italy): Detecting Ancient Harbour Remains. *Archaeological Prospection* 19,
1007 89–101. <https://doi.org/10.1002/arp.1420>
- 1008 Colombaroli, D., Marchetto, A., Tinner, W., 2007. Long term interactions between
1009 Mediterranean climate, vegetation and fire regime at Lago di Massaciuccoli (Tuscany,
1010 Italy). *Journal of Ecology* 95, 755–770. <https://doi.org/10.1111/j.1365-2745.2007.01240.x>
- 1012 Colombaroli, D., Vanniere, B., Emmanuel, C., Magny, M., Tinner, W., 2008. Fire-vegetation
1013 interactions during the Mesolithic-Neolithic transition at Lago dell'Accesa, Tuscany,
1014 Italy. *Holocene* 18, 679–692. <https://doi.org/10.1177/0959683608091779>
- 1015 Corrado, G., Amodio, S., Aucelli, P.P.C., Pappone, G., Schiattarella, M., 2020. The
1016 Subsurface Geology and Landscape Evolution of the Volturno Coastal Plain, Italy:
1017 Interplay between Tectonics and Sea-Level Changes during the Quaternary. *Water* 12,
1018 3386. <https://doi.org/10.3390/w12123386>
- 1019 Cosentino, C., Molisso, F., Scopelliti, G., Caruso, A., Insinga, D.D., Lubritto, C., Pepe, F.,
1020 Sacchi, M., 2017. Benthic foraminifera as indicators of relative sea-level fluctuations:
1021 Paleoenvironmental and paleoclimatic reconstruction of a Holocene marine succession

- 1022 (Calabria, south-eastern Tyrrhenian Sea). *Quaternary International* 439, 79–101.
1023 <https://doi.org/10.1016/j.quaint.2016.10.012>
- 1024 Delano Smith, C., 1976. The Tavoliere of Foggia (Italy): an aggradating coastland and its
1025 early settlement pattern. In: Davidson, D.A., Shackley, M.L. (eds.), *Geoarchaeology:*
1026 *Earth Science and the Past*. Duckworth, London, pp. 197–211.
- 1027 Delano Smith, C., Morrison, I.A., 1974. The buried lagoon and lost port of Sipontum
1028 (Foggia, Italy). *The International Journal of Nautical and Underwater Exploration* 3,
1029 275–281.
- 1030 De Santis, V., Caldara, M., 2015. The 5.5–4.5 kyr climatic transition as recorded by the
1031 sedimentation pattern of coastal deposits of the Apulia region, southern Italy. *The*
1032 *Holocene* 25, 1313–1329. <https://doi.org/10.1177/0959683615584207>
- 1033 De Santis, V., Caldara, M., Marsico, A., Capolongo, D., Pennetta, L., 2018. Evolution of the
1034 Ofanto River delta from the ‘Little Ice Age’ to modern times: Implications of large-
1035 scale synoptic patterns. *The Holocene* 28, 1948–1967.
1036 <https://doi.org/10.1177/0959683618798109>
- 1037 De Santis, V., Caldara, M., Torres, T. de, Ortiz, J.E., 2010. Stratigraphic units of the Apulian
1038 Tavoliere plain (Southern Italy): Chronology, correlation with marine isotope stages
1039 and implications regarding vertical movements. *Sedimentary Geology* 228, 255–270.
1040 <https://doi.org/10.1016/j.sedgeo.2010.05.001>
- 1041 De Santis, V., Scardino, G., Ortiz, J.E., Sánchez-Palencia, Y., Caldara, M., 2021. Pleistocene
1042 terracing phases in the metropolitan area of Bari - AAR dating and deduced uplift
1043 rates of the Apulian Foreland. *Rendiconti Online della Società Geologica Italiana* 54,
1044 49–61. <https://doi.org/10.3301/ROL.2021.03>
- 1045 De Santis, V., Caldara, M., Pennetta, L., 2020. “Continuous” Backstepping of Holocene
1046 Coastal Barrier Systems into Incised Valleys: Insights from the Ofanto and Carapelle-
1047 Cervaro Valleys. *Water* 12, 1799. <https://doi.org/10.3390/w12061799>
- 1048 De Venuto, G., Goffredo, R., Totten, D.M., 2022. Salapia-Salpi 1. Scavi e ricerche 2013-2016.
1049 Edipuglia, Bari, Italy.

- 1050 Di Donato, V., Esposito, P., Russo Ermolli, E., Scarano, A., Cheddadi, R., 2008. Coupled
1051 atmospheric and marine palaeoclimatic reconstruction for the last 35 ka in the Sele
1052 plain-gulf of Salerno area (southern Italy). *Quaternary International* 190, 146–157.
1053 <https://doi.org/10.1016/j.quaint.2008.05.006>
- 1054 Di Lorenzo, H., Aucelli, P., Corrado, G., De Iorio, M., Schiattarella, M., Russo Ermolli, E.,
1055 2021. Environmental evolution and anthropogenic forcing in the Garigliano coastal
1056 plain (Italy) during the Holocene. *The Holocene* 31, 1089–1099.
1057 <https://doi.org/10.1177/09596836211003242>
- 1058 Dini, M., Mastronuzzi, G., Sansò, P., 2000. The effects of relative sea level changes on the
1059 coastal morphology of Southern Apulia (Italy) during the Holocene. In: Slaymaker, O.
1060 (ed.), *Geomorphology, Human Activity and Global Environmental Changes*. Wiley,
1061 Chichester, UK, pp. 43–65.
- 1062 Di Rita, F., 2013. A possible solar pacemaker for Holocene fluctuations of a salt-marsh in
1063 southern Italy. *Quaternary International* 288, 239–248.
1064 <https://doi.org/10.1016/j.quaint.2011.11.030>
- 1065 Di Rita, F., Lirer, F., Bonomo, S., Cascella, A., Ferraro, L., Florindo, F., et al. 2018a. Late
1066 Holocene forest dynamics in the Gulf of Gaeta (central Mediterranean) in relation to
1067 NAO variability and human impact. *Quaternary Science Reviews* 179, 137–152.
1068 <https://doi.org/10.1016/j.quascirev.2017.11.012>
- 1069 Di Rita, F., Magri, D., 2009. Holocene drought, deforestation and evergreen vegetation
1070 development in the central Mediterranean: a 5500 year record from Lago Alimini
1071 Piccolo, Apulia, southeast Italy. *The Holocene* 19, 295–306.
1072 <https://doi.org/10.1177/0959683608100574>
- 1073 Di Rita, F., Magri, D., 2019. The 4.2 ka event in the vegetation record of the central
1074 Mediterranean. *Climate of the Past* 15, 237–251. [https://doi.org/10.5194/cp-15-237-](https://doi.org/10.5194/cp-15-237-2019)
1075 [2019](https://doi.org/10.5194/cp-15-237-2019)
- 1076 Di Rita, F., Molisso, F., Sacchi, M., 2018b. Late Holocene environmental dynamics,
1077 vegetation history, human impact, and climate change in the ancient Literna Palus
1078 (Lago Patria; Campania, Italy). *Review of Palaeobotany and Palynology* 258, 48–61.
1079 <https://doi.org/10.1016/j.revpalbo.2018.06.005>

- 1080 Di Rita, F., Simone, O., Caldara, M., Gehrels, W.R., Magri, D., 2011. Holocene
1081 environmental changes in the coastal Tavoliere Plain (Apulia, southern Italy): A
1082 multiproxy approach. *Palaeogeography, Palaeoclimatology, Palaeoecology* 310, 139-
1083 151. <https://doi.org/10.1016/j.palaeo.2011.06.012>
- 1084 Di Rita, F., Michelangeli, F., Celant, A., Magri, D., 2022. Sign-switching ecological changes
1085 in the Mediterranean Basin at 4.2 ka BP. *Global and Planetary Change* 208, 103713.
1086 <https://doi.org/10.1016/j.gloplacha.2021.103713>
- 1087 Doglioni, C., Mongelli, F., Pieri, P., 1994. The Puglia uplift (SE Italy): An anomaly in the
1088 foreland of the Apenninic subduction due to buckling of a thick continental
1089 lithosphere. *Tectonics* 13, 1309-1321. <https://doi.org/10.1029/94TC01501>
- 1090 Doglioni, C., Tropeano, M., Mongelli, F., Pieri, P., 1996. Middle-late Pleistocene uplift of
1091 Puglia: an anomaly in the Apenninic foreland. *Memorie della Società Geologica
1092 Italiana* 51, 101-117.
- 1093 D'Orefice, M., Bellotti, P., Bertini, A., Calderoni, G., Censi Neri, P., Di Bella, L., Fiorenza,
1094 D., Foresi, L.M., Louvari, M.A., Rainone, L., Vittori, C., Goiran, J.-P., Schmitt, L.,
1095 Carbonel, P., Preusser, F., Oberlin, C., Sangiorgi, F., Davoli, L., 2020. Holocene
1096 Evolution of the Burano Paleo-Lagoon (Southern Tuscany, Italy). *Water* 12, 1007.
1097 <https://doi.org/10.3390/w12041007>
- 1098 Emmanouilidis, A., Unkel, I., Triantaphyllou, M., Avramidis, P., 2020. Late-Holocene
1099 coastal depositional environments and climate changes in the Gulf of Corinth, Greece.
1100 *The Holocene* 30, 77-89. <https://doi.org/10.1177/0959683619875793>
- 1101 Fægri, K., Iversen, J., 1989. *Textbook of Pollen Analysis*, 4th Edition. John Wiley & Sons.
- 1102 Fiorentino, G., Caldara, M., De Santis, V., D'Oronzo, C., Muntoni, I. M., Simone, O.,
1103 Primavera, M., Radina, F., 2013. Climate changes and human-environment
1104 interactions in the Apulia region of southeastern Italy during the Neolithic period. *The
1105 Holocene* 23, 1297-1316. <https://doi.org/10.1177/0959683613486942>
- 1106 Florenzano, A., 2019. The History of Pastoral Activities in S Italy Inferred from
1107 Palynology: A Long-Term Perspective to Support Biodiversity Awareness.
1108 *Sustainability* 11, 404. <https://doi.org/10.3390/su11020404>

- 1109 Florenzano, A., Marignani, M., Rosati, L., Fascetti, S., Mercuri, A. M., 2015. Are Cichorieae
1110 an indicator of open habitats and pastoralism in current and past vegetation
1111 studies?. *Plant Biosystems – An International Journal Dealing with all Aspects of Plant*
1112 *Biology* 149, 154–165. <https://doi.org/10.1080/11263504.2014.998311>
- 1113 Gallicchio, S., Moretti, M., Spalluto, L., Angelini, S., 2014. Geology of the middle and
1114 upper Pleistocene marine and continental terraces of the northern Tavoliere di Puglia
1115 plain (Apulia, southern Italy). *Journal of Maps* 10, 569–575.
1116 <https://doi.org/10.1080/17445647.2014.895436>
- 1117 Ghilardi, M., Colleu, M., Pavlopoulos, K., Fachard, S., Psomiadis, D., Rochette, P., Demory,
1118 F., Knodell, A., Triantaphyllou, M., Delanghe-Sabatier, D., Bicket, A., Fleury, J., 2013.
1119 Geoarchaeology of Ancient Aulis (Boeotia, Central Greece): human occupation and
1120 Holocene landscape changes. *Journal of Archaeological Science* 40, 2071–2083.
1121 <https://doi.org/10.1016/j.jas.2012.12.009>
- 1122 Goffredo, R., 2014. Città, insediamenti rurali e paesaggi agrari della Daunia tra le guerre
1123 sannitiche e l'età post-annibalica. *BABESCH* 84, 47–73. doi:10.2143/BAB.89.0.3034669
- 1124 Goffredo, R., 2021. Salpi tra Medioevo ed Età Moderna: nascita, sviluppo e scomparsa di
1125 una città. *MEFRM* 133, 421–465. <https://doi.org/10.4000/mefrm.10098>
- 1126 Grimm, E.C., 1992. Tilia and Tilia-graph: pollen spreadsheet and graphics programs. In:
1127 8th International Palynological Congress, Aix-En- Provence, France, 6–12 September
1128 1992. p. 56.
- 1129 Haas, J.N., Richoz, I., Tinner, W., Wick, L., 1998. Synchronous Holocene climatic
1130 oscillations recorded on the Swiss Plateau and at timberline in the Alps. *The Holocene*
1131 8, 301–309. <https://doi.org/10.1191/095968398675491173>
- 1132 Hamilton, S., Whitehouse, R., 2021. Neolithic Spaces: Volume 1: Social and Sensory
1133 Landscapes of the First Farmers of Italy. *Specialist Studies on Italy*. Accordia Research
1134 Institute, University of London, London.
- 1135 Heim, J., 1995. Il paesaggio vegetativo. In: Mertens, J. (ed), *Herdonia. Scoperta di una città*.
1136 Bari, pp. 321–324.

- 1137 Hoffmann, J., 1961. Ergebnisse eines Anbauversuches mit Buchen verschiedener
1138 Herkunft in Tharandter Wald. Forstwissenschaftliches Centralblatt 80, 240–252.
1139 <https://doi.org/10.1007/BF01824386>
- 1140 Kornijów, R., Kowalewski, G., Sugier, P., Kaczorowska, A., Gasiorowski, M., Woszczyk,
1141 M., 2016. Towards a more precisely defined macrophyte-dominated regime: the recent
1142 history of a shallow lake in Eastern Poland. *Hydrobiologia* 772, 45–62.
1143 <https://doi.org/10.1007/s10750-015-2624-3>
- 1144 Lakhdar, R., Soussi, M., Ben Ismail, M.H., M'Rabet, A., 2004. A Mediterranean Holocene
1145 restricted coastal lagoon under arid climate: Case of the sedimentary record of Sabkha
1146 Boujmel (SE Tunisia). *Palaeogeography, Palaeoclimatology, Palaeoecology* 241, 177–
1147 191. <https://doi.org/10.1016/j.palaeo.2006.02.014>
- 1148 Lambeck, K., Antonioli, F., Anzidei, M., Ferranti, L., Leoni, G., Scicchitano, G., Silenzi, S.,
1149 2011. Sea level change along the Italian coast during the Holocene and projections for
1150 the future. *Quaternary International* 232, 250–257.
1151 <https://doi.org/10.1016/j.quaint.2010.04.026>
- 1152 Lintner, M., Biedrawa, B., Wukovits, J., Wanek, W., and Heinz, P., 2020. Salinity-
1153 dependent algae uptake and subsequent carbon and nitrogen metabolisms of two
1154 intertidal foraminifera (*Ammonia tepida* and *Haynesina germanica*), *Biogeosciences*, 17,
1155 3723–3732. <https://doi.org/10.5194/bg-17-3723-2020>
- 1156 Lippolis, E., Giammatteo, T., 2008. *Salpia vetus*. Archeologia di una città lagunare. Osanna
1157 Edizioni, Matera.
- 1158 López-Belzunce, M., Blázquez, A.M., Carmona, P., Ruiz, J.M., 2020. Multi proxy analysis
1159 for reconstructing the late Holocene evolution of a Mediterranean Coastal Lagoon:
1160 Environmental variables within foraminiferal assemblages. *CATENA* 187, 104333.
1161 <https://doi.org/10.1016/j.catena.2019.104333>
- 1162 Marchesini, M., Marvelli, S., Bandini Mazzanti, M., Accorsi, C.A., 1995. Ricerche
1163 archeoambientali nella Daunia antica. In: Quilici, L., Quilici Gigli, S. (eds), *Atlante*
1164 *tematico di topografia*. Suppl. 1, pp. 103–111.

- 1165 Marchiori, S., Medagli, P., Ruggiero, L., 1998. Guida botanica del Salento. Congedo
1166 Editore.
- 1167 Marin, M., 1973. Il problema delle tre "Salapia". *Archivio Storico Pugliese* 26, 365–388.
- 1168 Marin, M., 2018. Problemi riguardanti la stazione Salinis della Tabula Peutingeriana. In:
1169 Russo, S., Goffredo, R. (eds.), *Saline e sale nell'antichità, Atti del convegno sul Basso*
1170 *Tavoliere (1989), Bari*, pp. 81–90.
- 1171 Maselli, V., Trincardi, F., 2013. Large-scale single incised valley from a small catchment
1172 basin on the western Adriatic margin (central Mediterranean Sea). *Global and*
1173 *Planetary Change* 100, 245–262. <https://doi.org/10.1016/j.gloplacha.2012.10.008>
- 1174 Maselli, V., Trincardi, F., Asioli, A., Ceregato, A., Rizzetto, F., Taviani, M., 2014. Delta
1175 growth and river valleys: the influence of climate and sea level changes on the South
1176 Adriatic shelf (Mediterranean Sea). *Quaternary Science Reviews* 99, 146–163.
1177 <https://doi.org/10.1016/j.quascirev.2014.06.014>
- 1178 Mastronuzzi, G., Caputo, R., Di Bucci, D., Fracassi, U., Iurilli, V., Milella, M., Pignatelli, C.,
1179 Sansò, P., Selleri, G., 2011. Middle-Late Pleistocene evolution of the Adriatic coastline
1180 of the Southern Apulia (Italy) in response to relative sea-level changes. *Geografia*
1181 *Fisica e Dinamica Quaternaria* 34, 207–221.
- 1182 Mastronuzzi, G., Sansò, P., 2002a. Holocene coastal dune development and environmental
1183 changes in Apulia (southern Italy). *Sedimentary Geology* 150, 139–152.
1184 [https://doi.org/10.1016/S0037-0738\(01\)00272-X](https://doi.org/10.1016/S0037-0738(01)00272-X)
- 1185 Mastronuzzi, G., Sansò, P., 2002b. Holocene uplift rates and historical rapid sea-level
1186 changes at the Gargano promontory, Italy. *Journal of Quaternary Science* 17, 593–606.
1187 <https://doi.org/10.1002/jqs.720>
- 1188 Mazzini, I., Anadon, P., Barbieri, M., Castorina, F., Ferreli, L., Gliozzi, E., Mola, M., Vittori,
1189 E., 1999. Late Quaternary sea-level changes along the Tyrrhenian coast near Orbetello
1190 (Tuscany, central Italy): palaeoenvironmental reconstruction using ostracods. *Marine*
1191 *Micropaleontology* 37, 289–311. [https://doi.org/10.1016/S0377-8398\(99\)00023-7](https://doi.org/10.1016/S0377-8398(99)00023-7)
- 1192 Mazzini, I., Rossi, V., Da Prato, S., Ruscito, V., 2017. Ostracods in archaeological sites along
1193 the Mediterranean coastlines: three case studies from the Italian peninsula. In:

- 1194 Williams, M., Hill, T., Boomer, I., Wilkinson, I.P. (eds), The Archaeological and
1195 Forensic Applications of Microfossils: A Deeper Understanding of Human History.
1196 The Micropalaeontological Society, Special Publications. Geological Society, London,
1197 pp. 121–142.
- 1198 Meisch, C., 2000. Freshwater Ostracoda of Western and Central Europe. Spektrum
1199 Akademischer Verlag GmbH. Heidelberg, Berlin.
- 1200 Mercuri, A.M., Bandini Mazzanti, M., Florenzano, A., Montecchi, M.C., Rattighieri, E.,
1201 2013. *Olea*, *Juglans* and *Castanea*: the OJC group as pollen evidence of the development
1202 of human-induced environments in the Italian peninsula. Quaternary International
1203 303, 24–42. <https://doi.org/10.1016/j.quaint.2013.01.005>
- 1204 Miall, A.D., 1985. Architectural-element analysis: A new method of facies analysis applied
1205 to fluvial deposits. Earth-Science Reviews 22, 261–308. [https://doi.org/10.1016/0012-](https://doi.org/10.1016/0012-8252(85)90001-7)
1206 [8252\(85\)90001-7](https://doi.org/10.1016/0012-8252(85)90001-7)
- 1207 Miall, A.D., 2010. The Geology of Stratigraphic Sequences, 2nd ed. Springer, Berlin.
- 1208 Moore, P.D., webb, J.W., Collinson, M.E., 1991. Pollen analysis. BlackWell Scientific
1209 Publications, London.
- 1210 Muntoni, I.M., Delluniversità, E., Allegretta, I., Terzano, R., Eramo, G., 2022. Chert sources
1211 and Early to Middle Neolithic exploitation in the Tavoliere (Northern Apulia, Italy).
1212 Quaternary International 615, 43–65. <https://doi.org/10.1016/j.quaint.2021.01.016>
- 1213 Natali, C., Bianchini, G., 2018. Natural vs anthropogenic components in sediments from
1214 the Po River delta coastal lagoons (NE Italy). Environmental Science and Pollution
1215 Research 25, 2981–2991. <https://doi.org/10.1007/s11356-017-0986-y>
- 1216 Nichols, M.M., 1989. Sediment accumulation rates and relative sea-level rise in lagoons.
1217 Marine Geology 88, 201–219. [https://doi.org/10.1016/0025-3227\(89\)90098-4](https://doi.org/10.1016/0025-3227(89)90098-4)
- 1218 Noti, R., van Leeuwen, J.F.N., Colombaroli, D., Vescovi, E., Pasta, S., La Mantia, T., Tinner,
1219 W., 2009. Mid- and late-Holocene vegetation and fire history at Biviere di Gela, a
1220 coastal lake in southern Sicily, Italy. Vegetation History and Archaeobotany 18, 371–
1221 387. <https://doi.org/10.1007/s00334-009-0211-0>

- 1222 Orombelli, G., Pelfini, M., 1985. Una fase di avanzata glaciale nell'Olocene superiore,
1223 precedente alla Piccola Glaciazione, nelle Alpi Centrali. Rendiconti Società Geologica
1224 Italiana 8, 17–20.
- 1225 Patacca, E., Scandone, P., 2001. Late thrust propagation and sedimentary response in the
1226 thrust-belt – foredeep system of the Southern Apennines (Pliocene-Pleistocene). In:
1227 Vai, G.B., Martini, I.P. (eds.), Anatomy of an Orogen: The Apennines and Adjacent
1228 Mediterranean Basins. Springer Netherlands, Dordrecht, pp. 401–440.
1229 https://doi.org/10.1007/978-94-015-9829-3_23
- 1230 Pieri, P., Sabato, L., Tropeano, M., 1996. Significato geodinamico dei caratteri deposizionali
1231 e strutturali della Fossa bradanica nel Pleistocene. Memorie della Società Geologica
1232 Italiana 51, 501–515.
- 1233 Pieri, P., Festa, V., Moretti, M., Tropeano, M., 1997. Quaternary tectonic activity of the
1234 Murge area (Apulian foreland - Southern Italy). Annali di Geofisica XL, 1395–1404.
- 1235 Pieruccini, P., Susini, D., 2020. The Holocene sedimentary record and the landscape
1236 evolution along the coastal plains of the Pecora and Cornia rivers (Southern Tuscany,
1237 Italy): preliminary results and future perspectives. In: Bianchi, G., Hodges, R. (eds.),
1238 The NEU-Med Project: Vetricella, an Early Medieval Royal Property on Tuscany's
1239 Mediterranean. All'Insegna del Giglio, Firenze, pp. 161–168.
- 1240 Piva, A., Asioli, A., Trincardi, F., Schneider, R.R., Vigliotti, L., 2008. Late-Holocene climate
1241 variability in the Adriatic Sea (Central Mediterranean). The Holocene 18, 153–167.
1242 <https://doi.org/10.1177/0959683607085606>
- 1243 Pollegioni, P., Woeste, K., Chiocchini, F., Del Lungo, S., Ciolfi, M., Olimpieri, I., Tortolano,
1244 V., Clark, J., Hemery, G.E., Mapelli, S., Malvolti, M.E. 2017. Rethinking the history of
1245 common walnut (*Juglans regia* L.) in Europe: Its origins and human interactions. PLoS
1246 ONE 12, e0172541. <https://doi.org/10.1371/journal.pone.0172541>
- 1247 Primavera, D'Oronzo, C., Muntoni, I.M., Radina, F., Fiorentino, G., 2017. Environment,
1248 crops and harvesting strategies during the II millennium BC: Resilience and
1249 adaptation in socio-economic systems of Bronze Age communities in Apulia (SE Italy).
1250 Quaternary International 436, 83–95. <https://doi.org/10.1016/j.quaint.2015.05.070>

- 1251 Primavera, M., Simone, O., Fiorentino, G., Caldara, M., 2011. The palaeoenvironmental
1252 study of the Alimini Piccolo lake enables a reconstruction of Holocene sea-level
1253 changes in southeast Italy. *The Holocene* 21, 553–563.
1254 <https://doi.org/10.1177/0959683610385719>
- 1255 Reille, M., 1992. Pollen et spores d'Europe et d'Afrique du Nord. Laboratoire de Botanique
1256 Historique et Palynologie, Université d'Aix Marseille III, Marseille.
- 1257 Reille, M., 1995. Pollen et spores d'Europe et d'Afrique du Nord – Supplément 1.
1258 Laboratoire de Botanique Historique et Palynologie, Université d'Aix Marseille III,
1259 Marseille.
- 1260 Reille, M., 1998. Pollen et spores d'Europe et d'Afrique du Nord – Supplément 2.
1261 Laboratoire de Botanique Historique et Palynologie, Université d'Aix Marseille III,
1262 Marseille.
- 1263 Reimer, P.J., Austin, W.E.N., Bard, E., Bayliss, A., Blackwell, P.G., Bronk Ramsey, C.,
1264 Butzin, M., Cheng, H., Edwards, R.L., Friedrich, M., Grootes, P.M., Guilderson, T.P.,
1265 Hajdas, I., Heaton, T.J., Hogg, A.G., Hughen, K.A., Kromer, B., Manning, S.W.,
1266 Muscheler, R., Palmer, J.G., Pearson, C., Plicht, J. van der, Reimer, R.W., Richards,
1267 D.A., Scott, E.M., Southon, J.R., Turney, C.S.M., Wacker, L., Adolphi, F., Büntgen, U.,
1268 Capano, M., Fahrni, S.M., Fogtmann-Schulz, A., Friedrich, R., Köhler, P., Kudsk, S.,
1269 Miyake, F., Olsen, J., Reinig, F., Sakamoto, M., Sookdeo, A., Talamo, S., 2020. The
1270 IntCal20 Northern Hemisphere Radiocarbon Age Calibration Curve (0–55 cal kBP).
1271 *Radiocarbon* 62, 725–757. <https://doi.org/10.1017/RDC.2020.41>
- 1272 Ruello, M.R., Cinque, A., Donato, V. Di, Molisso, F., Terrasi, F., Russo Ermolli, E., 2017.
1273 Interplay between sea level rise and tectonics in the Holocene evolution of the St.
1274 Eufemia Plain (Calabria, Italy). *Journal of Coastal Conservation* 21, 903–915.
1275 <https://doi.org/10.1007/s11852-017-0558-9>
- 1276 Ruiz, F., Abad, M., Galán, E., González, I., Aguilá, I., Olías, M., Gómez Ariza, G.L.,
1277 Cantano, M., 2006. The present environmental scenario of El Melah Lagoon (NE
1278 Tunisia) and its evolution to a future sabkha. *Journal of African Earth Sciences* 44, 289–
1279 302. <https://doi.org/10.1016/j.jafrearsci.2005.11.023>

- 1280 Russo, G., Strizzi, C, 2013. La vegetazione del Parco Nazionale del Gargano (Promontorio
1281 del Gargano e Isole Tremiti). Atti del Congresso "Stelvio '70" 09/2005. Colloques
1282 Phytosociologiques, XXIX, 577–603.
- 1283 Russo Ermolli, E., Romano, P., Ruello, M.R., Barone Lumaga, M.R., 2014. The natural and
1284 cultural landscape of Naples (southern Italy) during the Graeco-Roman and late
1285 antique periods. *Journal of Archaeological Sciences* 42, 399–411.
1286 <https://doi.org/10.1016/j.jas.2013.11.018>
- 1287 Russo Ermolli, E., Ruello, M.R., Cicala, L., Di Lorenzo, H., Molisso, F., Pacciarelli, M., 2018.
1288 An 8300-yr record of environmental and cultural changes in the Sant'Eufemia plain
1289 (Calabria, Italy). *Quaternary International* 483, 39–56.
1290 <https://doi.org/10.1016/j.quaint.2018.01.033>
- 1291 Russo, S., 1985. La bonifica del lago Salpi in Capitanata. *L' Ambiente Storico*, 119–135.
- 1292 Sabatier, P., Dezileau, L., Barbier, M., Raynal, O., Lofi, J., Briquieu, L., Condomines, M.,
1293 Bouchette, F., Certain, R., Van Grafenstein, U., Jorda, C., Blanchemanche, P., 2010.
1294 Late-Holocene evolution of a coastal lagoon in the Gulf of Lions (South of France).
1295 *Bulletin de la Société Géologique de France* 181, 27–36.
1296 <https://doi.org/10.2113/gssgfbull.181.1.27>
- 1297 Sacchi, M., Molisso, F., Pacifico, A., Vigliotti, M., Sabbarese, C., Ruberti, D., 2014. Late-
1298 Holocene to recent evolution of Lake Patria, South Italy: An example of a coastal
1299 lagoon within a Mediterranean delta system. *Global and Planetary Change* 117, 9–27.
1300 <https://doi.org/10.1016/j.gloplacha.2014.03.004>
- 1301 Sadori, L., 2013. Southern Europe. In: Elias, S.A. (ed.), *The Encyclopedia of Quaternary*
1302 *Science*, vol. 4. Elsevier, Amsterdam, pp. 179–188.
- 1303 Sadori, L., Giardini, M., Gliozzi, E., Mazzini, I., Sulpizio, R., van Welden, A., Zanchetta, G.,
1304 2015. Vegetation, climate and environmental history of the last 4500 years at lake
1305 Shkodra (Albania/Montenegro). *The Holocene* 25, 435–444.
1306 <https://doi.org/10.1177%2F0959683614561891>

- 1307 Sadori, L., Giardini, M., Giraudi, C., Mazzini, I., 2010. The plant landscape of the imperial
1308 harbour of Rome. *Journal of Archaeological Science* 37, 3294–3305.
1309 <https://doi.org/10.1016/j.jas.2010.07.032>
- 1310 Sadori, L., Mazzini, I., Pepe, C., Goiran, J-P., Pleuger, E., Ruscito, V., Salomon, F., Vittori,
1311 C., 2016. Palynology and ostracodology at the Roman port of ancient Ostia (Rome,
1312 Italy). *The Holocene* 26, 1502–1512. <https://doi.org/10.1177/0959683616640054>
- 1313 Sadori, L., Giardini, M., 2007. Charcoal analysis, a method to study vegetation and climate
1314 of the Holocene: the case of Lago di Pergusa, Sicily (Italy). *Geobios* 40(2), 173–180.
1315 <https://doi.org/10.1016/j.geobios.2006.04.002>
- 1316 Sangiorgi, F., Capotondi, L., Nebout, N.C., Vigliotti, L., Brinkhuis, H., Giunta, S., Lotter,
1317 A.F., Morigi, C., Negri, A., Reichert, G.-J., 2003. Holocene seasonal sea-surface
1318 temperature variations in the southern Adriatic Sea inferred from a multiproxy
1319 approach. *Journal of Quaternary Science* 18, 723–732. <https://doi.org/10.1002/jqs.782>
- 1320 Santacroce, R., Cioni, R., Marianelli, P., Sbrana, A., Sulpizio, R., Zanchetta, G., Donahue,
1321 D.J., Joron, J.L., 2008. Age and whole rock–glass compositions of proximal pyroclastics
1322 from the major explosive eruptions of Somma-Vesuvius: A review as a tool for distal
1323 tephrostratigraphy. *Journal of Volcanology and Geothermal Research* 177, 1–18.
1324 <https://doi.org/10.1016/j.jvolgeores.2008.06.009>
- 1325 Siani, G., Magny, M., Paterne, M., Debret, M., Fontugne, M., 2013. Paleohydrology
1326 reconstruction and Holocene climate variability in the South Adriatic Sea. *Climate of*
1327 *the Past*, 9, 499–515. <https://doi.org/10.5194/cp-9-499-2013>
- 1328 Siani, G., Paterne, M., Arnold, M., Bard, E., Métivier, B., Tisnerat, N., Bassinot, F., 2000.
1329 Radiocarbon Reservoir Ages in the Mediterranean Sea and Black Sea. *Radiocarbon* 42,
1330 271–280. <https://doi.org/10.1017/S0033822200059075>
- 1331 Simeoni, U., 1992. I litorali di Manfredonia e Barletta (Basso Adriatico): Dissesti, sedimenti,
1332 problematiche ambientali. *Bollettino della Società Geologica Italiana* 111, 367–398.
- 1333 Smit, A., 1973. A scanning electron microscopical study of the pollen morphology in the
1334 genus *Quercus*. *Acta botanica neerlandica* 22, 655–665.

- 1335 Spagnoli, F., Bartholini, G., Dinelli, E., Giordano, P., 2008. Geochemistry and particle size
1336 of surface sediments of Gulf of Manfredonia (Southern Adriatic sea). *Estuarine,
1337 Coastal and Shelf Science* 80, 21–30. <https://doi.org/10.1016/j.ecss.2008.07.008>
- 1338 Stevenson, R.J., 1996. An Introduction to Algal Ecology in Freshwater Benthic Habitats. In:
1339 Stevenson, R.J., Bothwell, M., Lowe, R., Thorp J. (eds), *Algal Ecology. Freshwater
1340 Benthic Ecosystems. A volume in Aquatic Ecology*. Academic Press, p. 30.
- 1341 Stockmarr, J., 1971. Tablets with spores used in absolute pollen analysis. *Pollen et Spores*
1342 13, 615–621.
- 1343 Tafuri, M.A., Robb, J., Belcastro, M.G., Mariotti, V., Iacumin, P., Di Matteo, A., O'Connell,
1344 T., 2014. Herding Practises in the Ditched Villages of the Neolithic Tavoliere (Apulia,
1345 South-east Italy) A Vicious Circle? The Isotopic Evidence. In: Whittle, A., Bickle, P.
1346 (eds.), *Early Farmers: The View from Archaeology and Science, Proceedings of the
1347 British Academy*, vol. 198. Oxford University Press, Oxford, pp. 143–158.
- 1348 Tinner, W., van Leeuwen, J.F.N., Colombaroli, D., Vescovi, E., van der Knaap, W.O.,
1349 Henne, P.D., Pasta, S., D'Angelo, S., La Mantia, T., 2009. Holocene environmental and
1350 climatic changes at Gorgo Basso, a coastal lake in southern Sicily, Italy. *Quaternary
1351 Science Review* 28, 1498–1510. <https://doi.org/10.1016/j.quascirev.2009.02.001>
- 1352 Tinner, W., Colombaroli, D., Heiri, O., Henne, P.D., Steinacher, M., Untenecker, J., Vescovi,
1353 E., Allen, J.R.M., Carraro, G., Conedera, M., Joos, F., Lotter, A.F., Luterbacher, J.,
1354 Samartin, S., Valsecchi, V., 2013. The past ecology of *Abies alba* provides new
1355 perspectives on future responses of silver fir forests to global warming. *Ecological
1356 Monographs* 83, 419–439. <https://doi.org/10.1890/12-2231.1>
- 1357 Totten, D.M., 2022. Life in the Late Antique town: *Salapia* in the 4th-6th c. CE. In: De Venuto,
1358 G., Goffredo, R., Totten, D.M. (eds.), *Salapia-Salpi 1. Scavi e ricerche 2013-2016*.
1359 Edipuglia, Bari, Italy, pp. 629–660.
- 1360 Tropeano, M., Sabato, L., Pieri, P., 2002. Filling and cannibalization of a foredeep: the
1361 Bradanic Trough, Southern Italy. *Geological Society, London, Special Publications* 191,
1362 55–79. <https://doi.org/10.1144/GSL.SP.2002.191.01.05>

- 1363 Vacchi, M., Marriner, N., Morhange, C., Spada, G., Fontana, A., Rovere, A., 2016.
1364 Multiproxy assessment of Holocene relative sea-level changes in the western
1365 Mediterranean: Sea-level variability and improvements in the definition of the
1366 isostatic signal. *Earth-Science Reviews* 155, 172–197.
1367 <https://doi.org/10.1016/j.earscirev.2016.02.002>
- 1368 Volpe, G., 1990. *La Daunia nell'età della romanizzazione. Paesaggio agrario produzione e*
1369 *scambi. Adrias. Edipuglia, Bari.*
- 1370 Vignola, C., Bonetto, J., Furlan, G., Mazza, M., Nicosia, C., Russo Ermolli, E., Sadori, L.,
1371 2022. At the origins of Pompeii: the plant landscape of the Sarno River floodplain from
1372 the first millennium BC to the AD 79 eruption. *Vegetation History and Archaeobotany*
1373 31, 171–186. <https://doi.org/10.1007/s00334-021-00847-w>
- 1374 Walker, M., Head, M.J., Berkelhammer, M., Björck, S., Cheng, H., Cwynar, L., Fisher, D.,
1375 Gkinis, V., Long, A., Lowe, J., Newnham, R., Rasmussen, S.O., Weiss, H., 2018. Formal
1376 ratification of the subdivision of the Holocene Series/Epoch (Quaternary
1377 System/Period): two new Global Boundary Stratotype Sections and Points (GSSPs)
1378 and three new stages/subseries. *Episodes* 41, 213–223.
1379 <https://doi.org/10.18814/epiugs/2018/018016>
- 1380 Whitehouse, R., 2014. The chronology of the Neolithic ditched settlements of the Tavoliere
1381 and the Ofanto valley. *Accordia Research Paper* 13, 57–77.
- 1382 Whitlock, C., Higuera, P.E., McWethy, D.B., Briles, C.E., 2010. Paleoeological Perspectives
1383 on Fire Ecology: Revisiting the Fire-Regime Concept. *The Open Ecology Journal* 3, 6–
1384 23. <http://dx.doi.org/10.2174/1874213001003020006>
- 1385

1386 **List of figures:**

1387 **Figure 1.** Geological and geomorphological map of the study area modified from the on-
1388 line idro-geomorphological database of “Regione Puglia” (www.sit.puglia.it), and the
1389 National Geological Map from the “Istituto Superiore per la Ricerca Ambientale (ISPRA,
1390 www.isprambiente.gov.it). Datum: D_WGS_1984; GCS: WGS_1984_UTM_Zone_33N (as
1391 with all coordinates henceforth). Legend: 1) main towns; 2) boreholes; 3) archaeological
1392 sites; 4) water stream (natural/artificial channel); 5) alluvial fan; 6) carbonate Units
1393 (Mesozoic); 7) carbonate Units (Pliocene); 8) marine deposit – Middle Pleistocene; 9)
1394 alluvial deposit – Middle Pleistocene; 10) infralittoral deposit – Middle Pleistocene; 11)
1395 alluvial deposit – Middle/Upper Pleistocene; 12) alluvial deposit – Upper Pleistocene; 13)
1396 alluvial plain – Upper Pleistocene/Holocene; 15) beach deposit – Holocene; 16)
1397 reclamation deposit – Recent time; 17) artificial reservoir – Recent time (for interpretation
1398 of the references to colour in this figure legend, the reader is referred to the web version of
1399 this article, as for all figures henceforth).

1400 **Figure 2.** Salpi lagoon, location of the boreholes.

1401 **Figure 3.** Selection of depositional environments and sedimentary facies recognised in the
1402 Salpi cores. a) SAM9 core – poorly drained floodplain environment (AF1); b) SAM9 core –
1403 poorly drained floodplain (AF1) and crevasse splay (AF2); c) SAM4 core – partially drained
1404 floodplain (AF1) and channel log (AF3); d) SAM9 core – swamp-marshy environments
1405 (SMF1); e) SAM9 core – non-vegetated lagoonal environment (LBF1) and marginal
1406 vegetated lagoonal environment (LBF2).

1407 **Figure 4.** Grain size and micropalaeontological analyses of the SAM9 core. Densities of the
1408 identified ostracod species (using the OEG freshwater and euryhaline) and of the two most
1409 abundant foraminifera species *Hyantesina germanica* and *Ammonia tepida*. Occurrences of
1410 diatoms, carophytes, ehippia *Daphnia*-type and fish remains are also reported.

1411 **Figure 5.** Salpi lagoon, core SAM9. Percentage diagram of selected pollen and NPP taxa.
1412 Curves are exaggerated by a factor of 5x.

1413 **Figure 6.** Salpi lagoon, core SAM9. Concentration diagram of pollen, NPPs, and
1414 microcharcoals.

1415 **Figure 7.** Stratigraphic sequence of the Salapia cores with indication of the facies association
1416 and associated depositional environments.

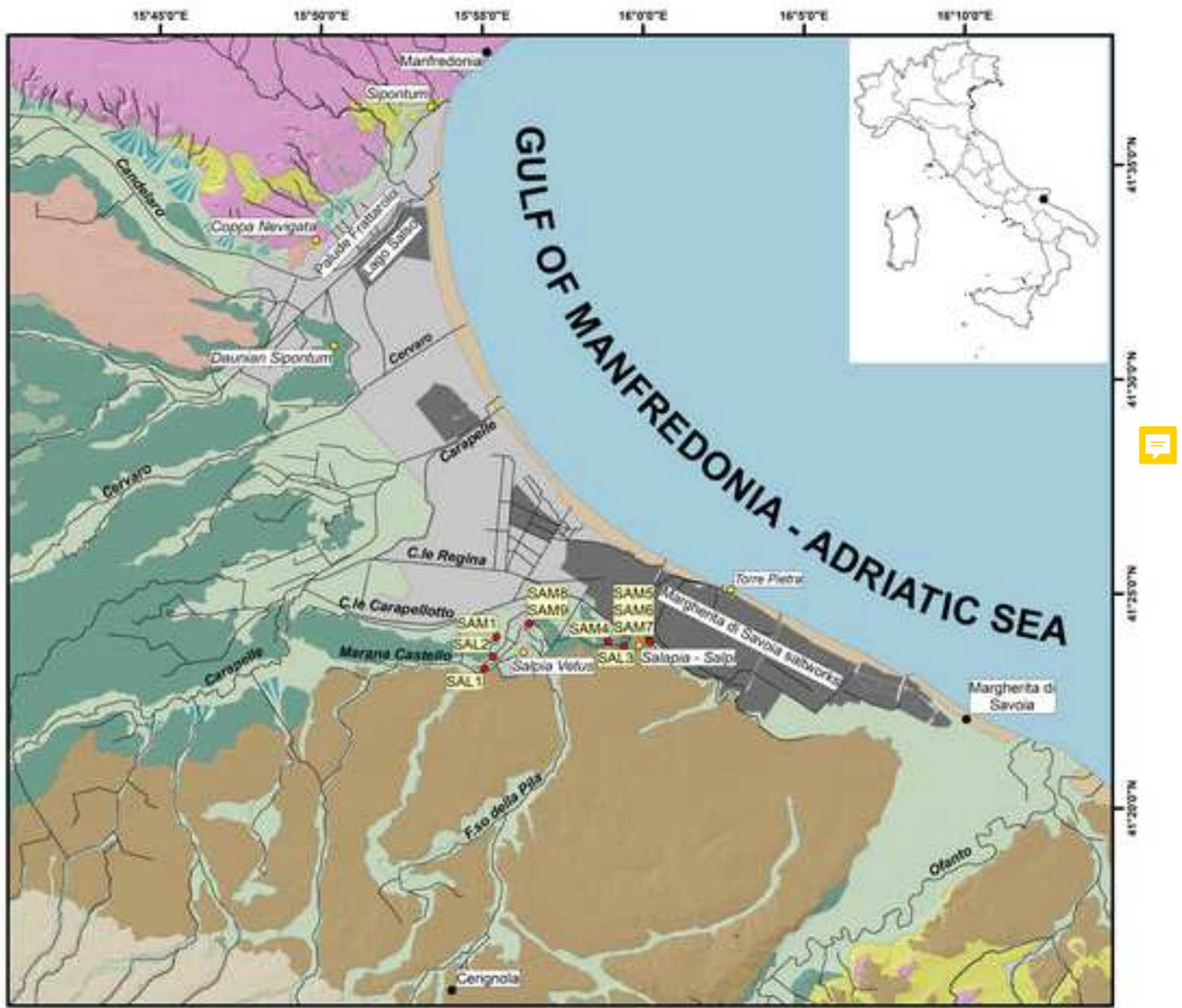
1417 **Figure 8.** Comparison between pollen and micropalaeontological data from the SAM9 core.
1418 The ecological groups of pollen, NPPs, and ostracods are aligned with the main
1419 palaeoenvironmental changes of the Salpi lagoon and with archaeological data from the
1420 Tavoliere plain. Halophytic herbs: *Amaranthaceae*; Riparian trees: *Alnus*, *Populus*, *Tamarix*;
1421 Xeric herbs: *Cichorieae*; Erosion indicators: *Glomus*, *Pseudoschizaea*; Algae: *Botryococcus*,
1422 *Pediastrum*, *Zygnemataceae*.

1423 **Figure 9.** Evolutionary model of the Salpi lagoon during the Holocene. a) Late
1424 Northgrippian (6.2ka - 4.2ka BP); b) Early Meghalayan (4.2ka - 2.4ka BP); c) Late
1425 Meghalayan (2.4ka BP - Present). Legend: 1) archaeological sites; 2) water streams; 3)
1426 alluvial fan; 4) carbonate Units - Mesozoic; 5) carbonate Units - Pliocene; 6) marine deposit
1427 - Middle Pleistocene; 7) alluvial deposit - Middle Pleistocene; 8) infralittoral deposit -
1428 Middle Pleistocene; 9) alluvial deposit - Middle/Upper Pleistocene; 10) alluvial deposit -
1429 Upper Pleistocene; 11) alluvial deposit - Upper Pleistocene/Holocene; 12) swamps deposit
1430 - Holocene; 13) Dune belts - Holocene; 14) Lagoon - Holocene.

1431 **List of tables:**

1432 **Table 1.** List of SAL and SAM boreholes.

1433 **Table 2.** List radiocarbon dating. Dating with asterisk in SAM9 core has been used for the
1434 age-depth model.

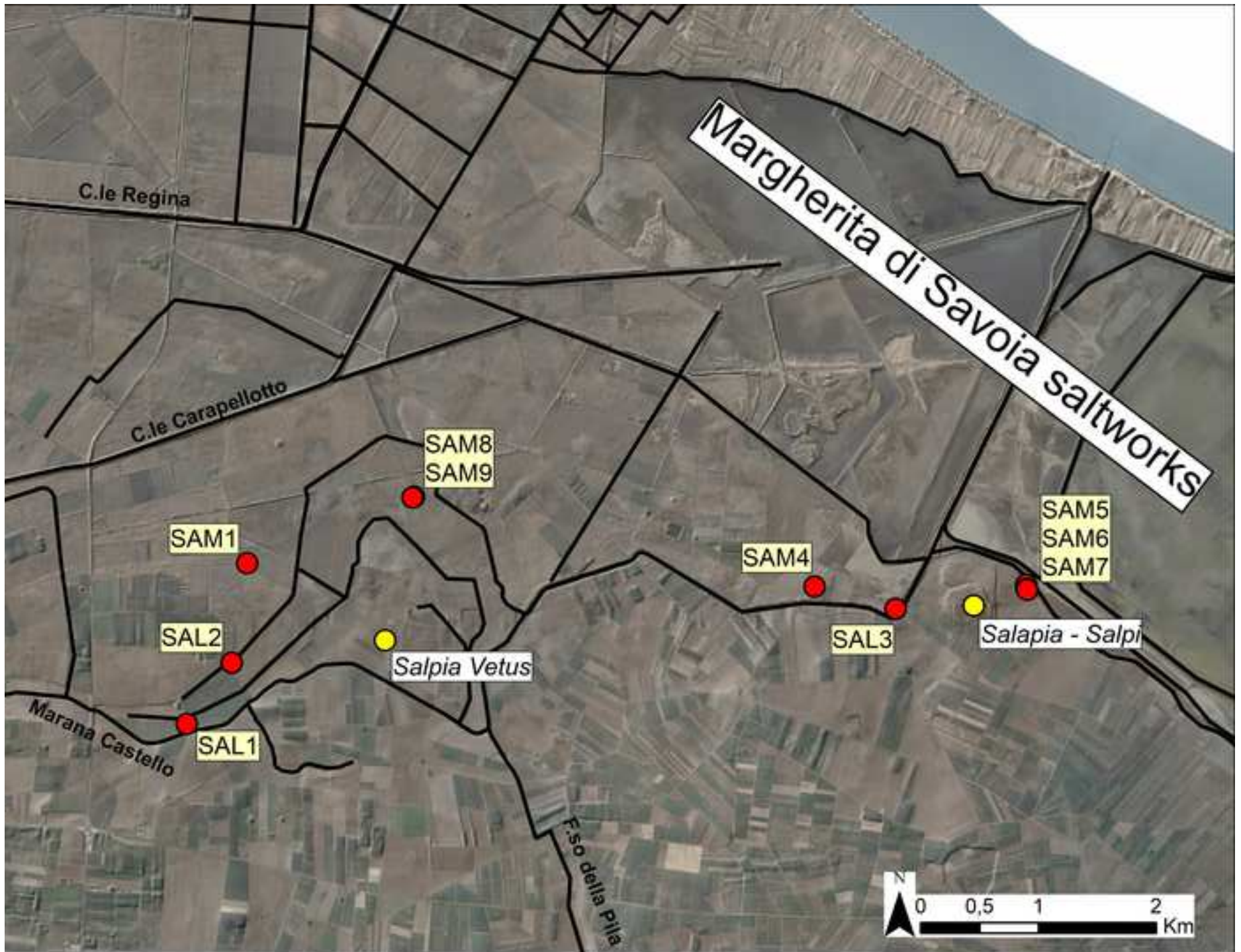


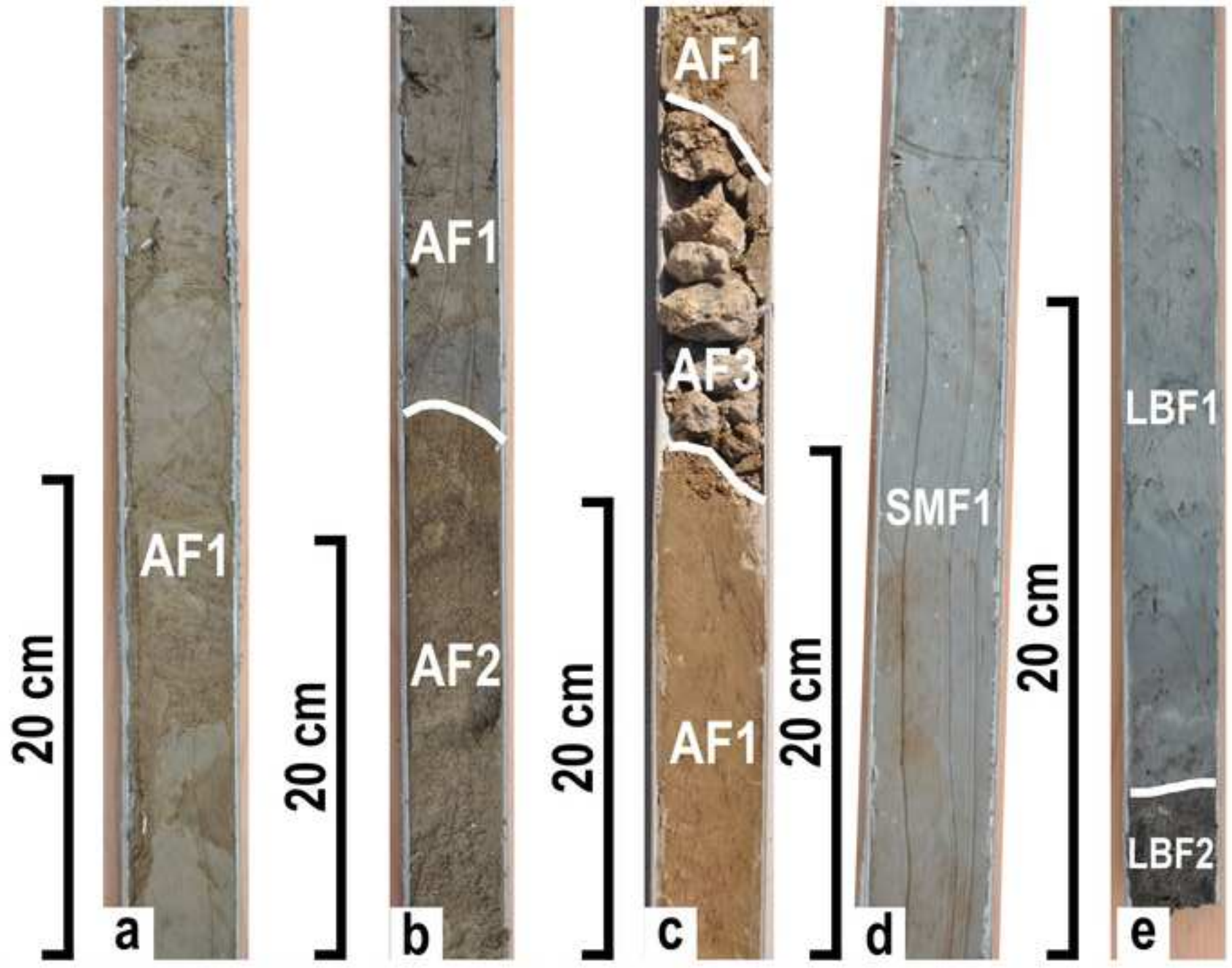
Tavoliere coastal plain - Salpi lagoon

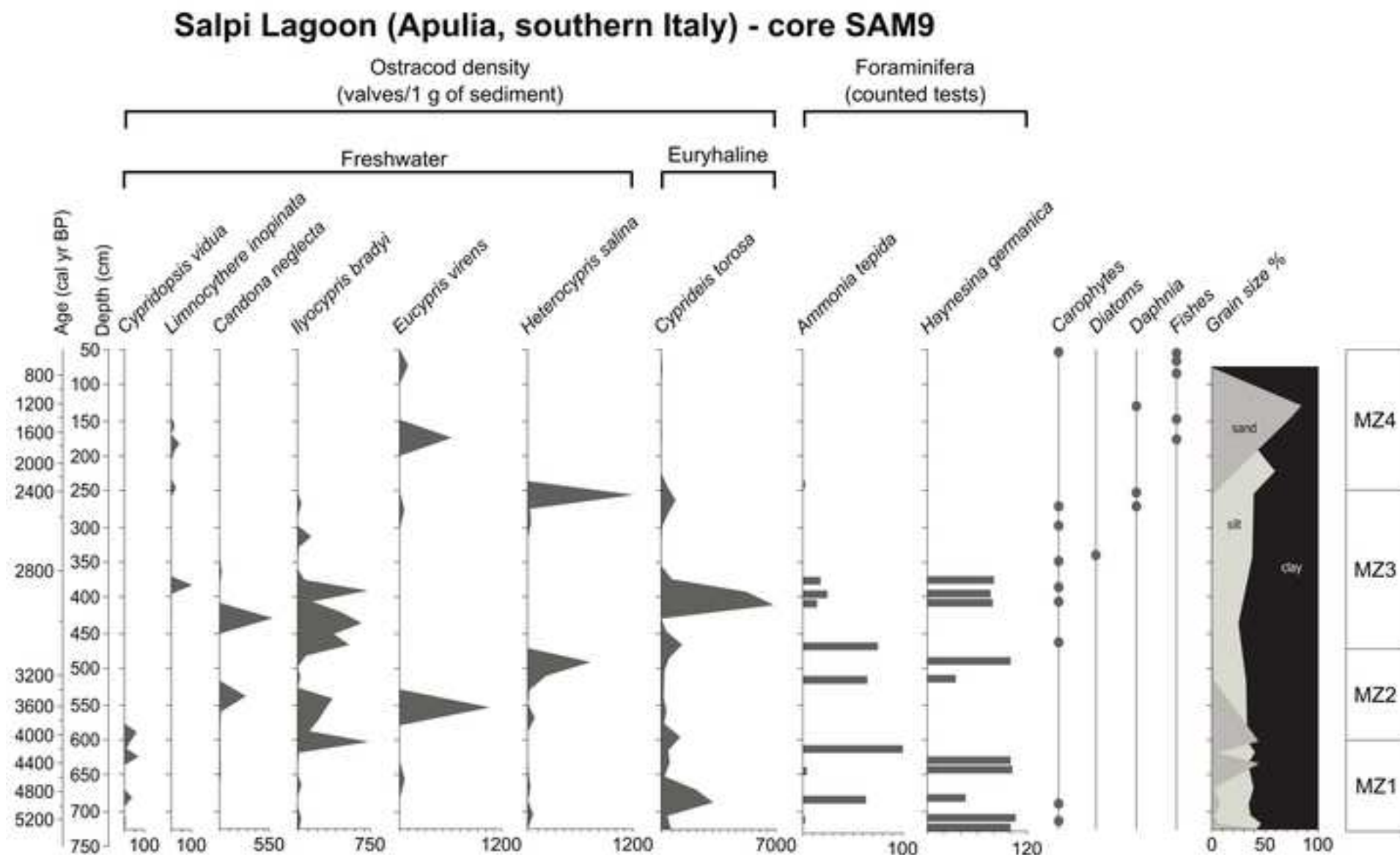
Legend

- | | | | | | | | |
|-----|------|------|------|------|------|------|------|
| ● 1 | ● 2 | ● 3 | — 4 | ▲ 5 | ■ 6 | ■ 7 | ■ 8 |
| ■ 9 | ■ 10 | ■ 11 | ■ 12 | ■ 13 | ■ 14 | ■ 15 | ■ 16 |

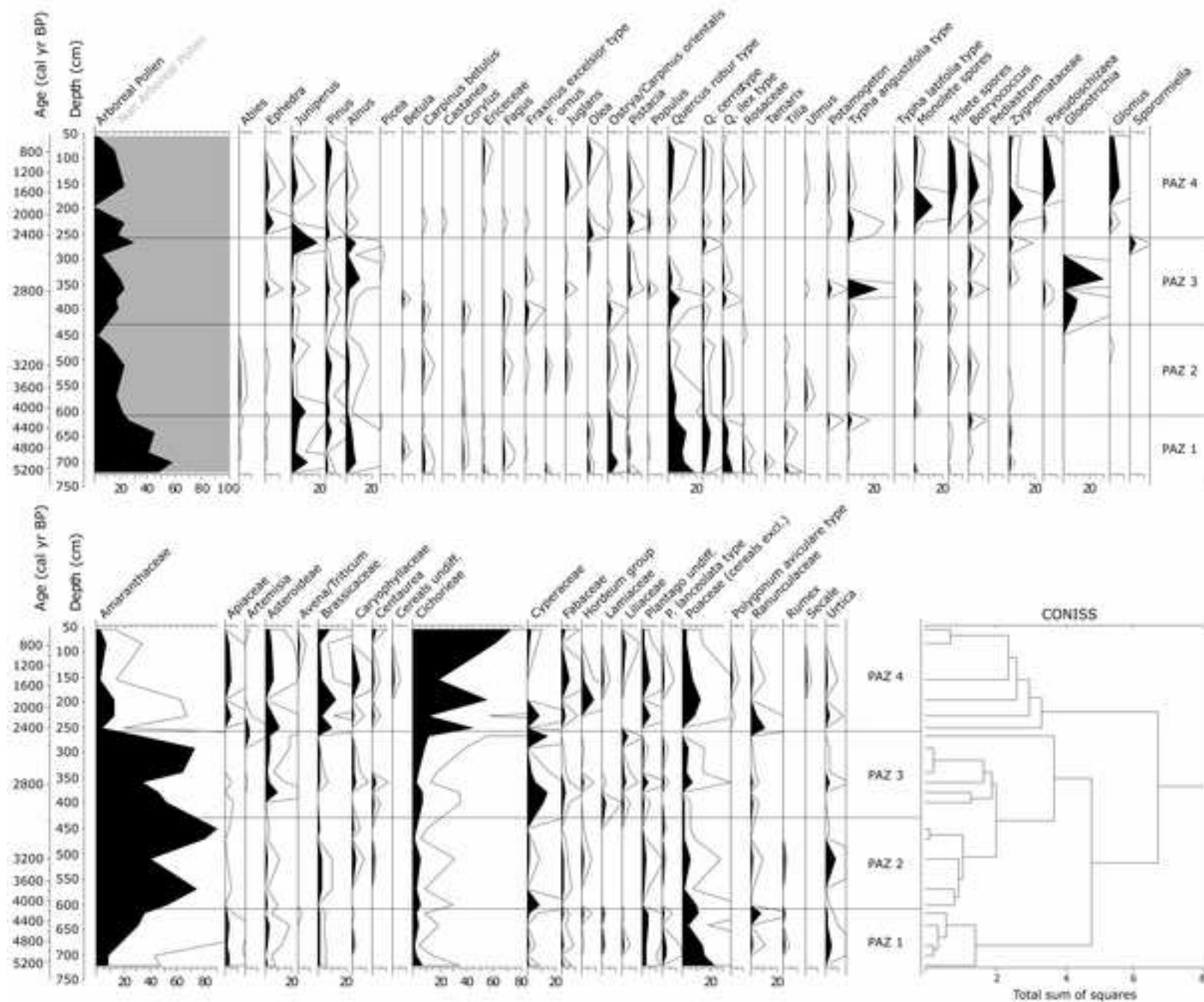
Figure 2







Salpi Lagoon (Apulia, southern Italy) core SAM9 - pollen percentage diagram



Salpi Lagoon (Apulia, southern Italy)
 core SAM9 - pollen concentration diagram

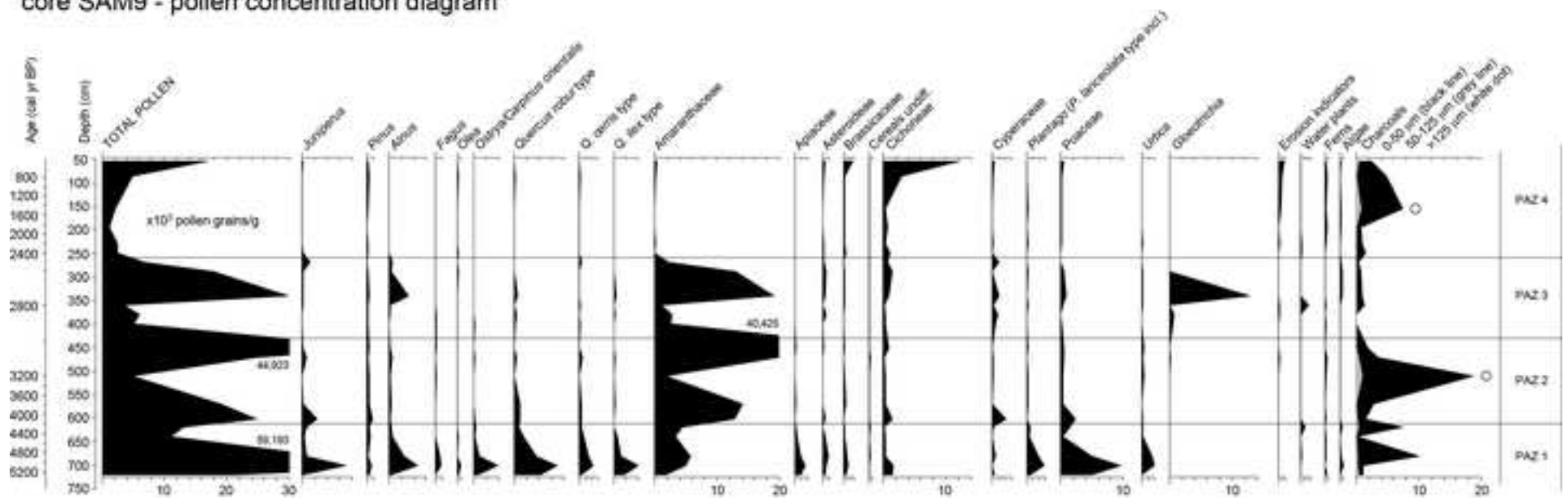


Figure 7

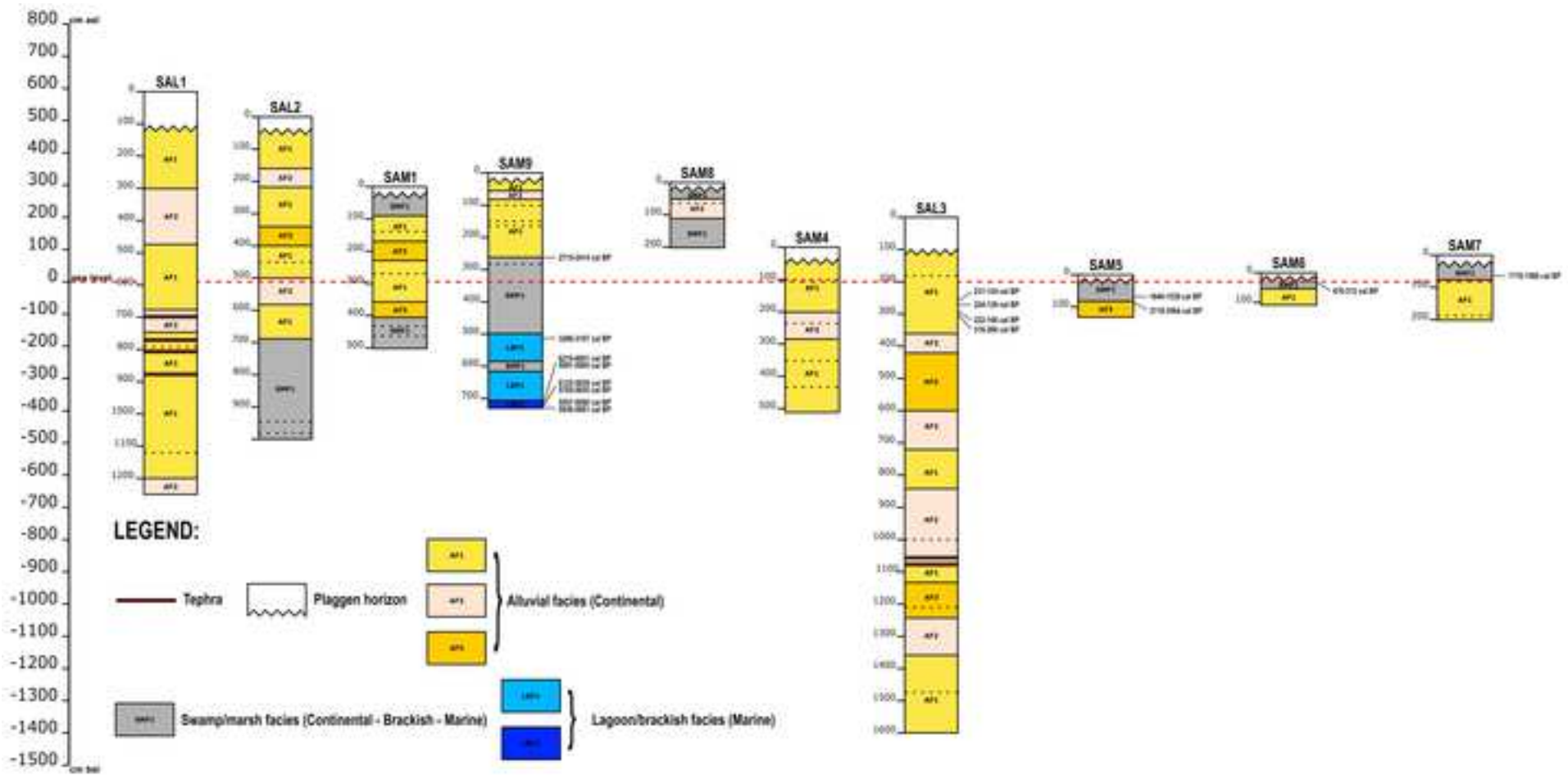
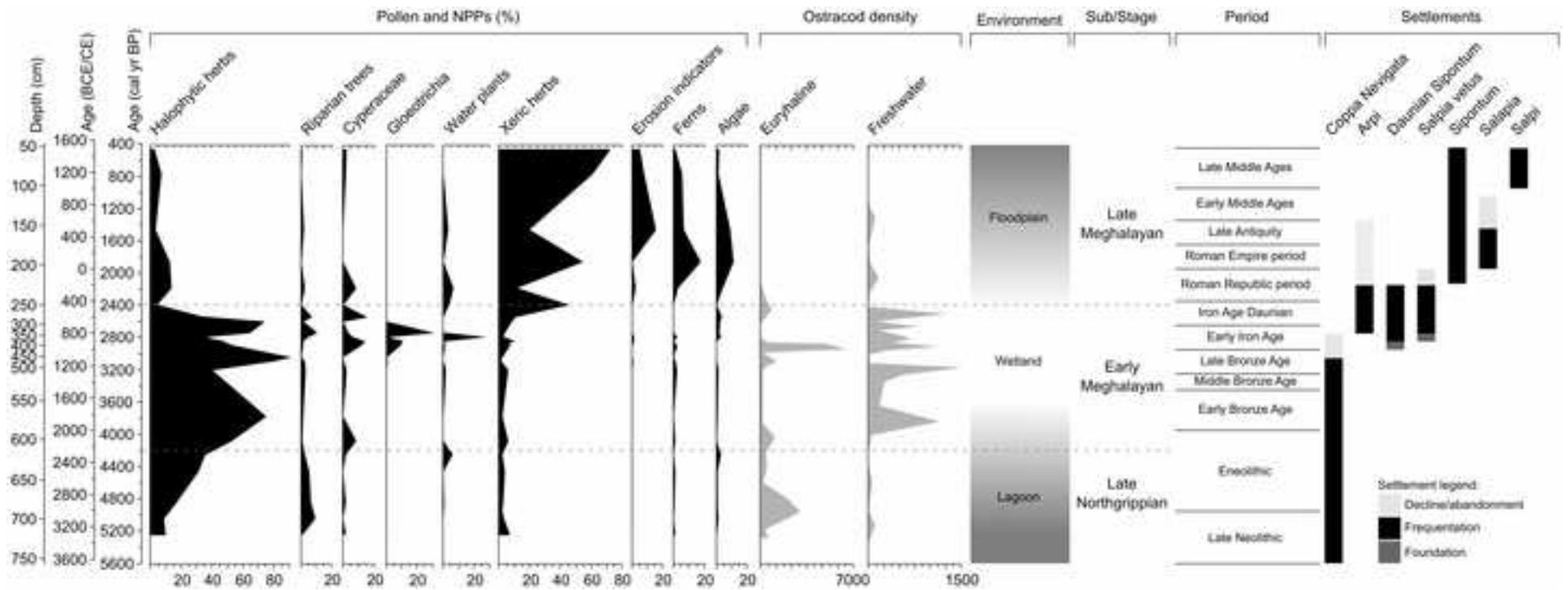
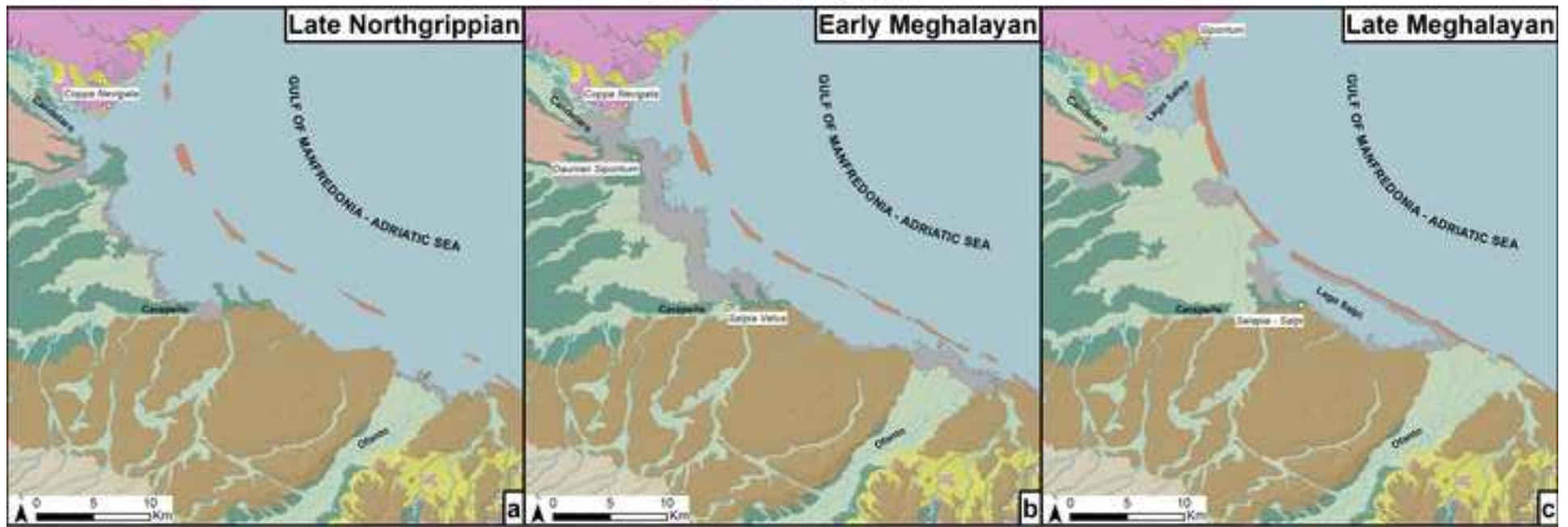


Figure 8



SALPI LAGOON



Legend



ID Borehole	year	Coordinates	Elevation (m asl)	Depth (m)
SAL1	2017	15°54'57,59"E, 41°23'16,82"N	5,9 m	12,5 m
SAL2	2017	15°55'24,175"E, 41°23'33,767"N	5,02 m	10 m
SAL3	2017	15°59'30,058"E, 41°23'43,196"N	2 m	16 m
SAM1	2019	15°55'28,709"E, 41°24'3,234"N	3 m	5 m
SAM4	2019	15°58'43,74"E, 41°23'57,147"N	1 m	5,2 m
SAM5	2019	15°59'59,058"E, 41°24'1,991"N	0,3 m	1,4 m
SAM6	2019	15°59'59,215"E, 41°24'0,952"N	0,4 m	1 m
SAM7	2019	15°59'59,469"E, 41°24'0,658"N	0,8 m	2,1 m
SAM8	2019	15°56'14,971"E, 41°24'28,036"N	3,1 m	2,1 m
SAM9	2019	15°56'15,575"E, 41°24'28,161"N	3,4 m	7,35 m

Core	ID-core depth (cm)	Material	Lab. Code	Age (BP)	Age cal. (BP)	Age cal. (BCE/CE)
SAL3	SAL3_260	Charcoal	Beta - 509119	160±30 BP	231 - 124 cal BP	1719 - 1826 cal CE
	SAL3_270	Charcoal	Beta - 509118	180±30 BP	224 - 136 cal BP	1726 - 1814 cal CE
	SAL3_290	Charcoal	Beta - 509117	200±30 BP	222 - 140 cal BP	1728 - 1810 cal CE
	SAL3_300	Charcoal	Beta - 509116	240±30 BP	318 - 268 cal BP	1632 - 1682 cal CE
SAM5	SAM5_65	Sediment	Beta - 595402	1720±30 BP	1640 - 1539 cal BP	310 - 410 cal CE
	SAM5_86	Sediment	Beta - 595401	3400±30 BP	3718 - 3564 cal BP	1769 - 1615 cal BCE
SAM6	SAM6_38	Sediment	Beta - 595403	340±30 BP	476 - 312 cal BP	1474 - 1638 cal CE
SAM7	SAM7_68	Sediment	Beta - 595404	1750±30 BP	1710 - 1566 cal BP	240 - 384 cal CE
SAM9	SAM9_262*	Sediment	Beta - 598710	2470±30 BP	2715 - 2414 cal BP	766 - 465 cal BCE
	SAM9_513*	Ostracod shell	Beta - 528223	3010±30 BP	3266 - 3107 cal BP	795 - 385 cal BCE
	SAM9_724a	Charcoal	Beta - 530035	5180±30 BP	5991 - 5905 cal BP	4042 - 3956 cal BCE
	SAM9_724b	Sediment	Beta - 528224	5340±30 BP	6210 - 6001 cal BP	4261 - 4052 cal BCE
	SAM9_727a	Charcoal	Beta - 528225	5010±30 BP	5765 - 5655 cal BP	3816 - 3706 cal BCE
	SAM9_727b	Sediment	Beta - 531708	5270±30 BP	6125 - 5939 cal BP	4176 - 3990 cal BCE
	SAM9_730a*	Ostracod shell	Beta - 531709	5180±30 BP	5557 - 5068 cal BP	3608 - 3119 cal BCE
	SAM9_730b	Sediment	Beta - 528226	5130±30 BP	5939 - 5861 cal BP	3990 - 3912 cal BCE